Land Degradation & Development

WILEY

RESEARCH ARTICLE OPEN ACCESS

Quantifying Soil Loss in the Brazilian Savanna Ecosystem: Current Rates and Anticipated Impact of Climate Changes

Dimaghi Schwamback[1,2] | Abderraman R. Amorim Brandão[1] | Luis Eduardo Bertotto[1] | Ronny Berndtsson[2] | Linus Zhang[2] | Edson Wendland[1] | Magnus Persson[2]

[1]Department of Hydraulics and Sanitation, São Carlos School of Engineering, University of São Paulo, São Paulo, Brazil | [2]Division of Water Resources Engineering, Department of Building and Environmental Technology, Lund University, Lund, Sweden

Correspondence: Dimaghi Schwamback (dimaghi.schwamback@tvrl.lth.se) | Magnus Persson (magnus.persson@tvrl.lth.se)

Received: 25 December 2023 | **Revised:** 24 July 2024 | **Accepted:** 20 September 2024

Funding: This study was funded in part by the Coordination for the Improvement of Higher Education Personnel (CAPES, Finance Code 001), in part by the Brazilian National Council for Scientific and Technological Development (CNPq), Ministry of Science, Technology and Innovation (MCTI), and São Paulo Research Foundation (FAPESP) (grant numbers 2015/03806-1, 2019/24292-7, 2021/14016-2, and 2023/08756-9).

Keywords: Brazil | Cerrado | erosion | land cover and land use | USLE

ABSTRACT

The Brazilian Savanna (Cerrado) is the second-largest South American biome that corresponds to almost two-third of the national agricultural production. Extensive agricultural-driven land-use changes have significantly altered the landscape, causing increased soil erosion. Furthermore, projections of climate change effects on the Cerrado raise concerns about the potential exacerbation of soil loss and its consequences on ecosystem sustainability. This study investigated soil loss for the Cerrado ecosystem by assessing current rates and projecting the potential effects of future climate change. Current soil loss was based on experimental plots (100 m^2) during 7 years maintained under typical main land cover in Brazil (sugarcane, pasture, Cerrado, and bare soil). Erosivity, by using the Universal Soil Loss Equation (USLE), was estimated from observations, parameters of erodibility, and land cover. To assess the future soil loss (2100), we used the calibrated USLE equation with yearly erosivity derived from 12 downscaled and bias-corrected SSP2-4.5 and SSP5-8.5 scenarios of CMIP6 climate model projections. Current agricultural practices induce considerable erosion, where sugarcane has 3.4 times higher soil loss as compared with the natural soil cover. Regarding future SSP2-4.5 and SSP5-8.5 scenarios (2100), we estimated an increase of 4.9% and 7.6% in soil loss, respectively, for all land covers. The observed soil loss rates underscore the critical importance of implementing sustainable land management practices to mitigate further soil degradation. Climate change may impose additional stress on the Cerrado ecosystem, amplifying the urgency for adaptive measures to safeguard this important biome.

1 | Introduction

Soil erosion is a severe form of land degradation, negatively impacting soil quality, biodiversity, food production, and water quality (Bagarello, Ferro, and Flanagan 2018; Roy et al. 2023). This degradation broadly affects the ecosystem functions and services provided by soil, vegetation, and water resource systems, ultimately threatening human well-being and the global climatic system (Prăvălie 2021). The main drivers of soil erosion by water are rainfall, land cover, land use, topography, and soil type. The intensification of soil loss is due to (i) changes in rainfall patterns and (ii) land use. The predicted alteration of rainfall patterns under future climate change scenarios, in terms of both amount and intensity, can potentially increase the disaggregation of soils (Amanambu et al. 2019; Duulatov et al. 2019; Weng et al. 2023). Population growth will escalate the demand for food, water, and energy, creating an imbalance between the supply and demand

of natural resources (Dawadi and Ahmad 2013; Veettil and Mishra 2020). Consequently, an increase of soil erosion due to changes in land use and land cover (LULC), primarily driven by deforestation and agricultural expansion is expected (Eekhout and de Vente 2022). Improving the understanding of relationships between land, hydrology, and climate is stated as one of the 23 major unsolved problems proposed by Bloschl et al. (2019).

Agriculture is a major driver of land use and cover changes globally (Aghsaei et al. 2020; Hailu, Mammo, and Kidane 2020), besides being the anthropogenic activity that constitutes the largest water use worldwide, representing 70% of the total freshwater withdrawal. Brazil is one of the global leaders in the export of agricultural and livestock derivative products, such as soybeans, corn, sugar, coffee, chicken, and beef (Stabile et al. 2020; Valdes, Hjort, and Seeley 2020). Although economically relevant, this has come with the loss of more than 70 Mha of natural vegetation from 1985 onward for agricultural and livestock production purposes (Souza et al. 2020). In Brazil, the productive engine for agricultural activities is mainly situated in the wooded Cerrado (WC) biome, situated in the center of the country, which supports 55% of the national meat production (Vendrame et al. 2010) and more than 50% of the productive agricultural areas (Spera 2017). The WC (or just Cerrado), is the Brazilian second largest ecoregion, covering an area equivalent to Germany, France, England, Italy, and Spain combined. Since the mid-twentieth century, the Cerrado has undergone agricultural expansion leading to a loss of almost 50% of the native forest vegetation (Strassburg et al. 2017) and less than 3% are conserved within protected areas (Costa Junior et al. 2012), which threatens not only the flora but also the fauna that dwells therein. This ecoregion has been declared as one of the 25 global biodiversity hotspots (Myers et al. 2000).

The extensive land-use changes driven by the agricultural expansion have altered the landscape, leading to changes in runoff patterns and increased soil loss (Oliveira et al. 2015; Anache et al. 2019), endangering water and food security. Soil erosion processes and their relationship with runoff and sediment concentration have been successfully evaluated worldwide in experimental field plots (Todisco et al. 2012; Lal et al. 2017; Chalise et al. 2020; Mohammed, Abdo, et al. 2020). Likewise, many mathematical models have been developed over time to estimate soil loss at the annual and event scales. The most widely model used is the empirical Universal Soil Loss Equation (USLE), elaborated by Wischmeier and Smith (1978) using runoff and soil loss data collected at the plot scale. To estimate the mean annual soil loss, USLE employs the product between five erosion-related factors: Rainfall erosivity, soil erodibility, topography, land cover, and management (Wischmeier and Smith 1978). Limitations of the USLE, primarily associated with its spatial (plot-scale) and temporal (mean annual) scales of application, as well as its use in regions with climate and landscape properties different from their development origin (Boardman 2006; Bagarello, Ferro, and Pampalone 2015), have prompted the development of several modified versions of the equation (e.g., Renard et al. 1997; Kinnell and Risse 1998; Bagarello et al. 2008). Still the original model remains an attractive tool for predicting soil erosion employing just a few parameters (Bagarello, Ferro, and Flanagan 2018), particularly relevant for practical applications in regions with scarce data such as Brazil.

There is an urgent need to consider future climatic alterations of soil loss estimation (Stefanidis and Stathis 2018; Aslan et al. 2019; Hateffard et al. 2021). For instance, rainfall erosivity, defined as the potential of rainfall to cause soil loss (Nearing et al. 2017), is expected to be affected by climate change (Biasutti and Seager 2015; Riquetti et al. 2020; Azari, Oliaye, and Nearing 2021; Panagos et al. 2022), varying in intensity locally. Consequently, the quantification of soil erosion under current and future scenarios is of major relevance to provide a basis for the adoption of mitigation strategies, especially over agricultural-natural hotspots such as the Cerrado biome. Despite numerous previous studies addressing erosivity and soil loss under climate change scenarios, most of them were based on simulations that lacked field monitoring for calibration of the historical period to enable accurate future predictions. Furthermore, proper evaluation of the linkages between land degradation and climate change is fundamental for the development of soil erosion mitigation policies and building climate-resilient agroecological systems (Webb et al. 2017), which aligns with the objectives of the UN's 17 Sustainable Development Goals.

The present study aimed to investigate the change in soil loss resulting from changes in LULCs within the Cerrado biome and climate change until the end of the century. For that, we (i) calibrated the USLE model based on current soil loss monitoring and (ii) estimated soil loss under future climate change scenarios. Measured data from experimental plots (100 m^2) over 7 years maintained under typical main land covers found in Brazil (sugarcane, pasture, WC, and bare soil) were used to estimate the parameters of the USLE model. To assess the future soil loss (up to 2100), we implemented the calibrated USLE equation with yearly erosivity derived from climate data by the CLIMBbra (Ballarin et al. 2023), a Brazilian dataset based on the SSP2–4.5 and SSP5–8.5 scenarios of CMIP6 climate model projections. Our findings are unique and to the best of our knowledge, the first study to use downscaled (regional) bias-corrected climate models of the sixth generation (CMIP6, O'Neill et al. 2016; Tebaldi et al. 2021) for soil loss evaluation, contributing to anticipation of the impacts of climate change on soil loss in the WC biome.

2 | Materials and Methods

In Figure 1 is given the summary of the methodological flowchart employed in this study, composed of three phases. The first phase comprehends the field monitoring of soil loss and rainfall (intensity and amount) where a higher description is given in Section 2.1. In the second phase, the field data is employed to estimate and calibrate the parameters that compose the soil loss model (USLE). Greater details about the model handling are given in Section 2.2, while Section 2.4 details the statistical tools employed to evaluate model performance. Lastly, to investigate the implications of climate change on soil loss at the intermediate and distant future periods, regional climate models (RCMs) were handled and applied to the calibrated USLE

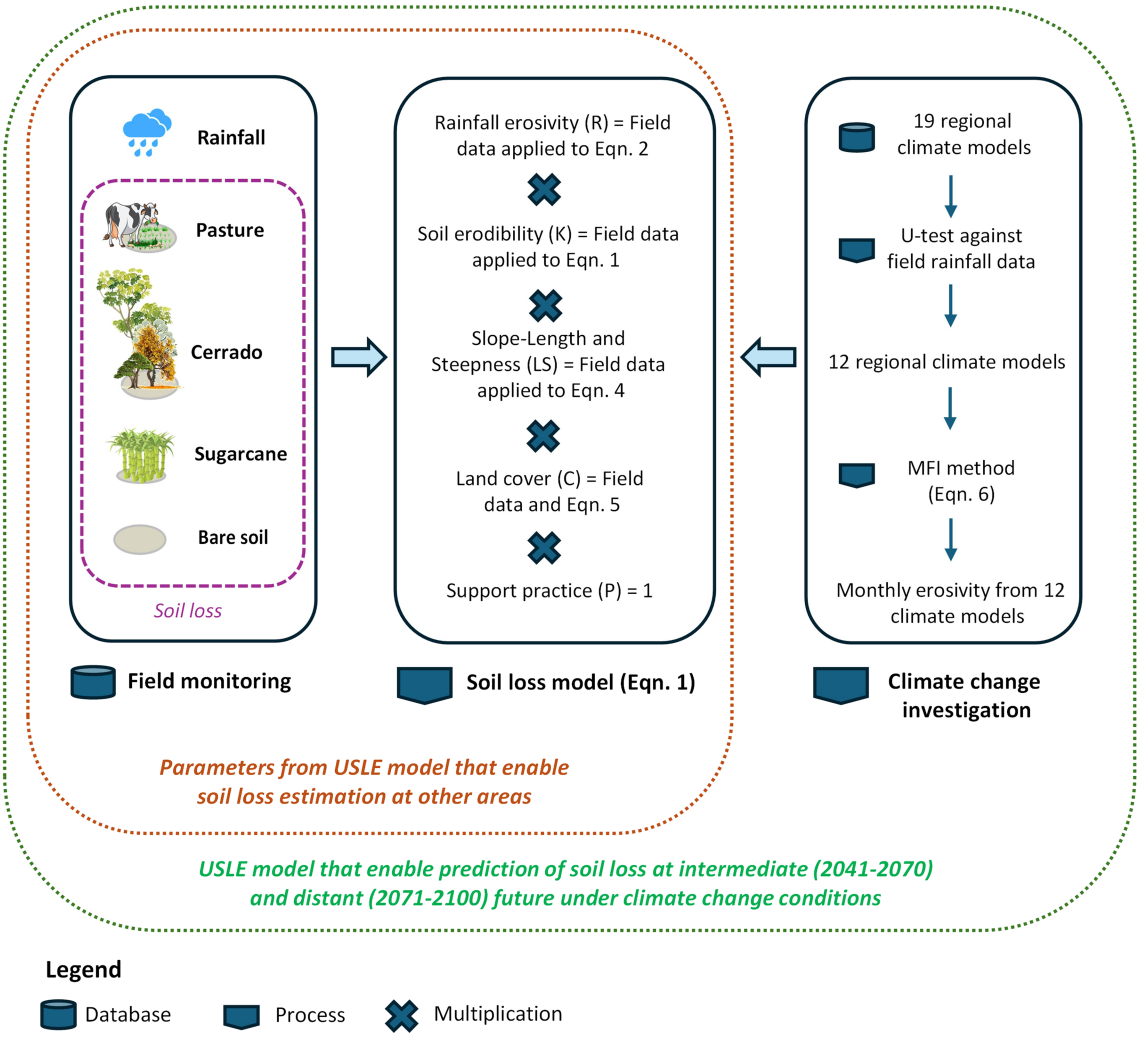

FIGURE 1 | Methodological flowchart employed in this study. [Colour figure can be viewed at wileyonlinelibrary.com]

model. Further methodological details regarding phase 3 are given in Section 2.3.

2.1 | Study Area and Soil Loss Observations

The field monitoring site is located at the Fazenda São José (22°10′S, 47°52′W), Instituto Arruda Botelho (IAB), in the municipality of Itirapina, São Paulo State, Southeast region of Brazil (Figure 2). The area is inside two major hydrological, environmental, and agricultural hotspots in the country: the Guarani Aquifer System (Oliveira et al. 2021) outcrop zone and the WC biome. The WC biome, also known as the Brazilian savanna, is home to trees with unique physiological adaptations that enable them to thrive in its challenging environment. The flora is not homogeneous, but instead composed of a mosaic of more than 4000 small, tortuous, 6–7 m high tree species (Cima, Amaral, and Massi 2023). These trees possess deep root systems to access water during dry seasons, a thick cork on their trunks, stiff leathery leaves, and xeromorphic characteristics to reduce water loss (Ribeiro and Walter 2008). Lastly, the defined dry seasons over 6 months are prone to wildfires and tree adaptations to fire include thick bark for protection and the ability to resprout from roots or lower stems after damage (Santos et al. 2024).

According to the Koppen classification system (Alvares et al. 2013), the climate in the region is humid subtropical (Cwa), with dry winter (April to September) and a hot humid summer. Considering the rainy season, our yearly analysis started on July 1st. The average altitude is 780 m and the average annual precipitation is 1248 mm (see Table 3), with a mean temperature of 21.6°C and relative humidity of 71% (Oliveira, Nearing, and Wendland 2015). From the Brazilian soil classification system (SiBCS), the soil in the study area is classified as Ortic Quartzarenic Neosol (RQo) with sandy texture (EMBRAPA 1997), poor in nutrients and acidic type. In Table 1 is given the pedological characteristics of the study area based on analysis of a sample resulted from the mix of three samples collected inside each plot.

The study area comprises experimental plots with 100 m^2 (20 m long and 5 m wide) with 9% slope gradient delimited by 30 cm high metal sheets. The plots were designed in triplicates to adequately represent field variation and covered by four typical LULCs commonly found in the Southeast region of Brazil: sugarcane (SC), pasture (PS), and bare soil (BS) at Site 1, and WC remnant area at Site 2. Since the implementation of the experimental plots in 2011 (Oliveira, Nearing, and Wendland 2015; Youlton, Bragion, and Wendland 2016; Youlton et al. 2016),

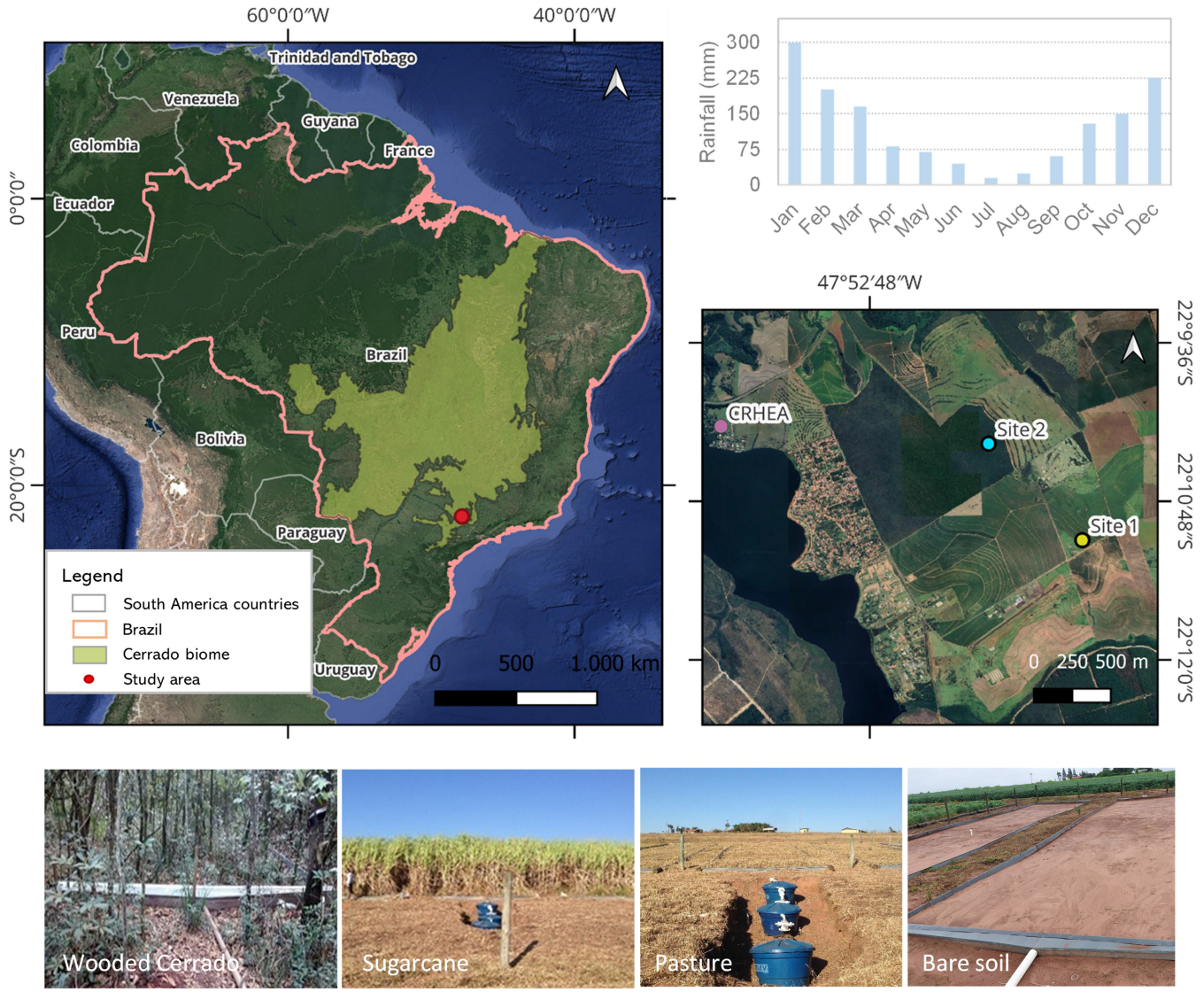

FIGURE 2 | Study sites location, monthly rainfall distribution, and photos of experimental plots. [Colour figure can be viewed at wileyonlinelibrary.com]

TABLE 1 | Pedological characteristics of the study area.

Depth (cm)	Bulk density ($g\,cm^{-3}$)	Sand (%)	Silt (%)	Clay (%)	pH	Particle density ($g\,cm^{-3}$)	Hydraulic conductivity ($mm\,h^{-1}$)
15	1.399	85	4	11	4.73	—	—
30	1.499	83	4	13	4.55	2.64	147.31
60	1.495	81	5	14	4.52	2.65	117.01
90	1.501	81	8	12	4.33	2.65	129.34

continuous monitoring of runoff and soil erosion has been carried out for each of the land covers (Anache et al. 2018; Anache et al. 2019). Besides runoff and soil loss observations, located beside plots at site 1 there is an automatic weather station (IAB station) collecting meteorological data (precipitation, relative humidity, temperature, solar radiation, wind speed, and direction) at 10 min resolution. Close to site 1 (5.2 km) another weather station (CRHEA station) provides similar meteorological observations since 1973, but at a daily resolution. The IAB station data were employed during calculation of erosivity, modified Fournier index (MFI), and USLE model under the current time-frame, while CRHEA was used for climate change model selection since it has a longer data record covering the baseline of the climate model.

Surface runoff carrying soil particles flows downstream in the plot and is collected by a gutter made of metal sheets, then directed through an outlet toward water tanks of 310-L capacity. The soil loss was assessed gravimetrically in the laboratory. The soil, collected in the water tanks, was quantified by multiplying

the content in 1 L water samples collected simultaneously with measurements of water levels within the storage tanks. The gravimetric technique was applied to determine the dry mass of soil, which did not make its way to the storage tanks. Consequently, the complete soil loss following a rainfall event was calculated by adding the dry mass of soil retained within the collection units and the outcome of multiplying the sediment concentration by the runoff volume. The field monitoring dataset employed is freely available at https://zenodo.org/doi/10.5281/zenodo.10009738 while wider data description is given by Schwamback et al. (2024).

2.2 | Universal Soil Loss Equation

The USLE, developed by Wischmeier and Smith (1978), was used to estimate and predict soil loss in current and future climate scenarios. The USLE is a well-established, worldwide used equation to estimate the average annual soil loss related to sheet and rill erosion occurrence, being composed by six factors representative of climate (R), soil (K), topography (LS), vegetation (C), and management aspects (P):

$$A = R \cdot K \cdot LS \cdot C \cdot P \tag{1}$$

where A is the mean annual soil loss per unit area ($t\,ha^{-1}\,year^{-1}$), R is the rainfall erosivity factor ($MJ\,mm\,ha^{-1}\,h^{-1}$), K is the soil erodibility factor ($t\,ha\,h\,ha^{-1}\,MJ^{-1}\,mm^{-1}$), L is the slope-length factor (dimensionless), S is the slope-steepness factor (dimensionless), C is the cover and management factor (dimensionless), and P is the support practice factor (dimensionless).

2.2.1 | Rainfall Erosivity Factor (R)

The rainfall erosivity is related to the kinetic energy of falling raindrops that detach soil particles, which enhances their transport rate with runoff (Renard et al. 1997; Mohammed, Alsafadi, et al. 2020). Calculation of R can be made for annual and other periods (Nearing et al. 2017). In this study, the R factor was calculated using the Rainfall Intensity Summarization Tool (RIST, USDA 2013). The rainfall erosivity index for each storm, spanning from July 2012 to June 2019, was expressed by Equation (2):

$$R = \sum_{i=1}^{n}\left(\sum_{j=1}^{m} e_j \times v_j\right) \times I_{30i} \tag{2}$$

where n is the total number of rainfall events during the period of interest, E_i represents the kinetic energy of the rainfall event ($MJ\ ha^{-1}$), and I_{30i} is the maximum 30-min intensity of the rainfall event ($mm\,h^{-1}$). For the kinetic energy calculation, e_j is the kinetic energy of the raindrop ($MJ\,ha^{-1}\,mm^{-1}$), v_j is the precipitation depth of the raindrop (mm), and m is the total number of raindrops in the event. The kinetic energy of each raindrop, which is a distinguishing factor in the USLE (Nearing et al. 2017), is defined by Brown and Foster (1987) as:

$$e_j = 1099\left[1 - 0.72\exp(-1.27i)\right] \tag{3}$$

where e_j is the unitary kinetic energy ($MJ\,ha^{-1}\,mm^{-1}$) and i is the raindrop intensity ($mm\,h^{-1}$).

To compute the R factor that is related to soil loss, it is essential to define the minimum inter-event time (MIT) during which rainfall periods are considered to be isolated and non-erosive. Rainfall events separated by MITs of no precipitation can influence the erosivity calculations of the defined storms (Tu et al. 2023). Several studies have segregated rainfall events based on different intervals, such as 1 (Molina-Sanchis et al. 2016), 4 (Tu et al. 2023), 6 (Nearing et al. 2017; Oliveira, Nearing, and Wendland 2015), and 12 h (Bracken and Croke 2007). To select the most appropriate MIT we correlated monthly soil loss and MIT ranging from 0.5 to 24 h and found that 6 h was the most suitable (Data S1), which is higher than the minimum 1 h MIT required for drainage in macropores to influence antecedent soil moisture and runoff (Molina-Sanchis et al. 2016). Therefore, events were considered isolated when the precipitation was less than 1 mm over 6 h MIT and erosive when it was higher than 10 mm (Tu et al. 2023).

2.2.2 | Slope-Length Factor (LS)

The LS factor represents the slope-length (L) and slope-steepness (S) of the regional topography for soil erosion rates (Ghosal and Das Bhattacharya 2020). By convenience, they are often used as a single topographic factor, namely the LS factor (Wischmeier and Smith 1978). The LS factor is determined based on the length and slope of the plot (Equation (4), McCool et al. 1987):

$$LS = \frac{\lambda^m}{22.1} \times 0.065 + 0.045s + 0.0065s^2 \tag{4}$$

where, λ (m) represents the plot length, s is the slope (%), and m is a parameter exponent (equals to 0.5 for slopes higher than 5%, 0.4 for slopes ranging from 3.5% to 4.5%, 0.3 for slopes spanning 1% to 3%, and 0.2 for consistent gradients below 1%).

2.2.3 | Crop Management Factor

The cover and management (C) factor indicates the protection efficiency of a particular vegetation cover from soil erosion (Bing and Lei 2022; Hou et al. 2020). Thus, this factor represents the relation between phenological (e.g., canopy cover and dry matter production) and management (e.g., tillage and soil cover) characteristics by environmental data, such as rainfall (Rocha and Sparovek 2021). The computation of the cover and management factor (C-factor) involved the assessment of the 322 erosive storms that occurred between July 2012 and June 2020. This parameter was derived by comparing the soil loss from each treatment to observation from bare soil (soil loss ratio, SLR), and by accounting for the portion of the erosive rainfall occurring during that time interval compared with the sum of erosivity (Wischmeier and Smith 1978):

$$C = \frac{SLR_1 \times EI30_1 + SLR_2 \times EI30_2 + \ \ldots \ + SLR_n \times EI30_n}{\sum_{i=1}^{n} EI30_i} \tag{5}$$

where SLR_i is the average soil loss observed in vegetated replicated plots divided by the average soil loss observed in replicated plots under bare soil, and EI_{30} is the erosivity at event i.

2.2.4 | Soil Erodibility Factor (K)

The soil erodibility (K) factor describes the soil particles' susceptibility to detachment and transport by water. Hence, it is as factor that reflects the soil composition and sensitivity to be exposed to erosion (Zhu et al. 2019; Atoma, Suryabhagavan, and Balakrishnan 2020), being primarily influenced by soil texture, but also structure, organic matter, and permeability. Here, K was determined based on the simplification of Equation (1), given by mean soil loss (A) divided by the rainfall erosion index (R), since LS (topography), C (soil cover and management), and P (support practices) have a value of 1 if soil erodibility is assessed in a fallow standard experimental plot that is not managed with support practices (Anache et al. 2015).

2.2.5 | Conservation Support Practice Factor (P)

The support practice (P) factor is related to the impact of land use and certain farming and tillage-supporting practices on soil erosion (Pham, Degener, and Kappas 2018). Regarding agriculture practices, the adoption of strategies to control soil erosion, such as contouring, terracing, and strip-cropping has a significant impact on soil loss through the P factor (Nyesheja et al. 2019). Since the plots did not employ any conservation practice, this factor was equal to 1.

2.3 | Climate Change Models

To estimate the future soil loss, we employed the USLE equation with the same factors (C, K, and LS-factors) as described above. The rainfall erosivity (R) was calculated using rainfall data from the CLIMBra—Climate Change Dataset for Brazil (Ballarin et al. 2023). ClimBRA offers 19 CMIP6 RCMs bias-corrected daily rainfall at 0.25° spatial resolution. The simulations encompassed a baseline period (1980–2013) and a future period (2015–2100), each propelled by two Shared Socioeconomic Pathways (SSPs): the middle-of-the-road scenario (SSP2–4.5, updated RCP4.5 pathway) and the path characterized by fossil-fueled expansion (SSP5-8.5, updated RCP8.5 pathway). The latter scenario embodies the upper limit of forthcoming trajectories, involving emissions substantial enough to achieve a radiative forcing of 8.5 W m^{-2} by the year 2100. In contrast, SSP2-4.5 represents the intermediate segment within the spectrum of forthcoming pathways by achieving a radiative forcing of 4.5 W m^{-2} by the year 2100. These two scenarios represent an updated iteration of the previous RCPs as outlined in CMIP5 (RCP4.5 and RCP8.5). We chose these two SSPs first because the scenarios encompass a broad spectrum of projected alterations in global climate dynamics and second, they hold the distinction of being the most frequently utilized future outlooks in Brazilian studies related to climate change (Almagro et al. 2017; Ballarin et al. 2023). This second prominence is particularly evident in projects led by the climatological institution in the country (National Institute for Space Research—INPE), which furnishes future data simulated by RCMs by incorporating the two corresponding RCPs-CMIP5.

Even though the climate models available by CLIMBra were bias-corrected with national historical data, there might be local differences in rainfall patterns that could interfere with the erosivity calculations. To avoid this, the Mann–Whitney U test was used for comparing monthly median differences between baseline data from each model and local historical observations from the CRHEA weather monitoring station. The U-test does not assume any specific distribution (such as normal distribution of samples) for calculating test statistics and p values. From the 19 models available at CLIMBra, we selected 12 RCMs (Table 2).

Since the climate model projections provide daily records and RIST required sub-daily records, to construct the erosivity we used the relationship between monthly R from local observations and the MFI (Arnoldus 1977), given by Equation (6). We employed three different curve fitting methods including linear, logarithmic, and power function to identify the one with the highest correlation with historical erosivity.

$$MFI = \sum_{i=1}^{12} \frac{p_i^2}{P} \tag{6}$$

where p_i represents the rainfall (mm) of the ith month, and P denotes the total annual rainfall (mm).

2.4 | Statistical Model Performance

Model performance of representing monitored soil loss was evaluated in terms of coefficient of determination (R^2, Equation 7), Percent of Bias (PBIAS, Equation 8), and Root Mean Squared Error (RMSE, Equation 9):

$$R^2 = 1 - \left(\frac{\sum_{i=1}^{N} \left(y_{i,\text{pred}} - y_{i,\text{obs}}\right)^2}{\sum_{i=1}^{N} \left(y_{i,\text{obs}} - \bar{y}_{i,\text{obs}}\right)^2} \right), 0.0 < R^2 \leq 1 \tag{7}$$

$$\text{PBIAS} = \frac{\sum_{i=1}^{N} \left(y_{i,\text{obs}} - y_{i,\text{pred}}\right)}{\sum_{i=1}^{N} y_{i,\text{obs}}} \times 100, 0.0 < \text{PBIAS} < \infty \tag{8}$$

$$\text{RMSE} = \sqrt{\frac{1}{N} \sum_{i=1}^{N} \left(y_{i,\text{pred}} - y_{i,\text{obs}}\right)^2}, 0.0 < \text{RMSE} < \infty \tag{9}$$

wherein N is the sample size, y_{pred} and y_{obs} are the predicted and observed data, respectively, $\bar{y}_{\text{obs}}$ is the mean value of the observed data. RMSE shares the data's units, PBIAS is given in percentage, and R^2 is dimensionless.

3 | Results

3.1 | USLE Parameters

Soil loss was mainly driven by the land cover factor (Pearson of 0.81, p value < 0.05), followed by soil erodibility with moderate significant correlation (Pearson of 0.51, p value < 0.05), while rainfall

TABLE 2 | Bias-corrected CMIP6 climate model projections used for climate projection based on the SSP2–4.5 and SSP5–8.5 scenarios.

Model	Country/ Region	Reference	*p*-value *U* test	RMSE[a]	PBIAS[a]
ACCESS-CM2	Australia	Bi et al. (2020)	0.61	112.97	0.23
ACCESS-ESM1-5	Australia	Law et al. (2017); Ziehn et al. (2020)	0.15	104.81	−0.20
EC-EARTH3	Europe	Doscher et al. (2022)	0.77	91.60	0.35
GFDL-CM4	USA	Held et al. (2019)	0.77	100.00	0.22
GFDL-ESM4	USA	Dunne et al. (2020)	0.18	111.42	−0.10
HadGEM3-GC31-LL	UK	Williams et al. (2018)	0.21	103.96	−0.13
K-ACE	South Korea	Lee et al. (2020)	0.51	110.71	0.28
MIROC6	Japan	Tatebe et al. (2019)	0.34	97.40	0.56
MPI-ESM1-2	Germany	Gutjahr et al. (2019); Müller et al. (2018)	0.57	97.63	−0.32
MRI-ESM2	Japan	Yukimoto et al. (2019)	0.34	101.89	−0.12
NESM3	China	Cao et al. (2018)	0.14	114.21	−0.11
UKESM1.0	UK	Sellar et al. (2019)	0.36	98.61	−0.04

[a]Metric based on comparing model historical precipitation (1980–2013) and field observations.

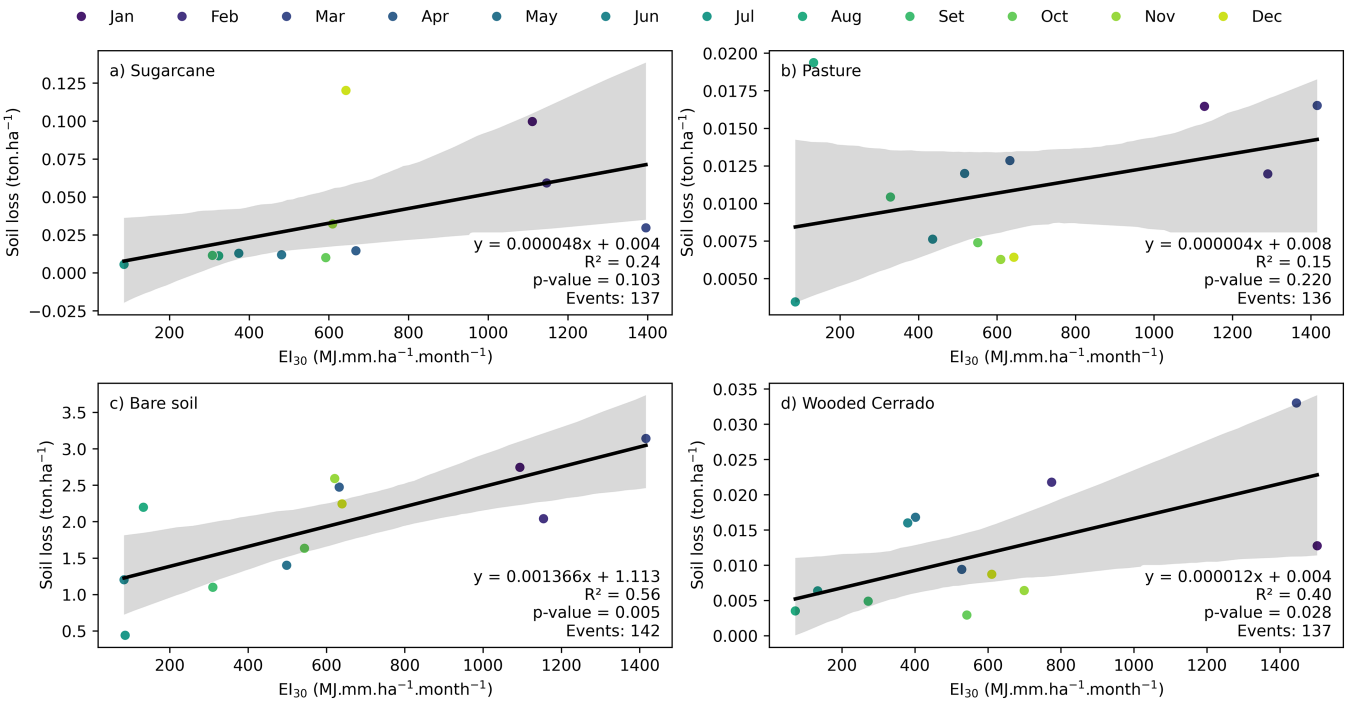

FIGURE 3 | Scatter of monthly soil loss events based on correspondent rainfall erosivity. The gray area indicates the 95% confidence interval of fitting curve. [Colour figure can be viewed at wileyonlinelibrary.com]

erosivity did not exhibit a statistically significant relationship (Pearson of −0.07, p value < 0.05). In the following paragraph, further explanations of each USLE parameter are performed.

3.1.1 | Erosivity Factor (*R*)

Over the past 7 years, 1057 isolated rainfall events were monitored, with 322 erosive (23.4%) and 1057 nonerosive (76.6%) events. Note that rainfall events in August were nonerosive based on criteria implemented in RIST (see Table 3 monthly distribution of rainfall and erosivity). The study area had a rainy season between December and March that accounted for 52% of mean annual erosivity whereas the dry season (Jun–Aug) corresponded to approximately 1.3% of annual erosivity. From Figure 3 we can see the relationship between rainfall erosivity and soil loss for each treatment analyzed. Soil losses for BS ($R^2 = 0.56$) and WC ($R^2 = 0.40$) plots strongly depended on

TABLE 3 | Monthly erosivity (ton ha^{-1} year^{-1}) and erosivity density monitored at study area location.

Month	Precipitation (mm)	Erovivity (MJ mm ha^{-1} h)	Erosivity density (MJ ha^{-1} h)
Jan	204.13	1001.63	4.91
Feb	154.62	1000.55	6.47
Mar	131.13	709.83	5.41
Apr	74.78	281.04	3.76
May	75.97	321.23	4.23
Jun	36.12	44.08	1.22
Jul	18.48	15.11	0.82
Aug	24.91	0	0
Sep	66.41	153.42	2.31
Oct	112.35	482.36	4.51
Nov	159.23	481.21	3.02
Dec	197.32	713.64	3.62
Total	1255.45	5204.10	4.15

erosivity (p value < 0.05), while SC ($R^2 = 0.24$) and PS ($R^2 = 0.15$) plots had a nonsignificant dependence (p value > 0.05). Comparing soil management practices in agricultural areas, sugarcane has annual seasonal practices (i.e., tillage) while seasonal compaction occurs during pasture rotation of cattle. These activities impact soil porosity, structure, and permeability which lead to a unique sensitivity to rainfall erosivity.

3.1.2 | Soil Erodibility (*K*) and Slope-Length Factors (*LS*)

Based on the ratio between mean annual soil loss at bare soil plot and annual erosivity, we obtained an erodibility for the Neossolo soil equal to 0.0027982 ton ha h ha^{-1} MJ^{-1} mm^{-1}. Considering the experimental plot size and slope, the *LS* factor was equal to 0.9526.

3.1.3 | Land Cover Factor (*C*)

The land cover factor for sugarcane, pasture, and WD was 0.0286, 0.0123, and 0.0133, respectively. These values demonstrate a major difference in erosion vulnerability among agricultural land uses, where sugarcane had a 2.3-fold higher potential soil loss than pasture. This difference was expected and can be attributed, among other factors, to the soil disturbance practices for the sugarcane-covered plot and greater soil compaction due to cattle trampling in the pasture-covered plot. When comparing the *C* factor from agricultural (mean values of pasture and sugarcane) and natural (WC) covered plots, the former had a 1.5-fold smaller soil loss potential, due to the permanent deep root system that enables infiltration and forest litter to prevent rainfall splash with following soil particle transport.

3.2 | Actual Soil Loss Estimated by USLE

The monitored annual soil loss and estimation by USLE for each treatment are presented in Figure 4. From the observed means, bare soil resulted in the highest soil loss (18.8 ton ha^{-1}), followed by sugarcane (0.41 ton ha^{-1}), and WC (0.12 ton ha^{-1}), while pasture (0.1 ton ha^{-1}) had the lowest one. As expected, soil particles in bare soil areas are easily detached and without organic barriers they are easily removed by runoff, leading to higher soil losses. Sugarcane presented greater soil loss than pasture due to the higher soil disturbance caused by tillage and plantation (Anache et al. 2018). In addition, pasture areas had a greater aggregation of soil particles due to their fasciculated roots that enhance soil resistance to erosion (Nacinovic et al. 2014). On the other hand, native forest had lower monitored soil loss since it is composed of a complex number of herbal species with deep root systems that promote fast infiltration, and thick litter that reduce splash effects and subsequent soil particle transport (Siqueira et al. 2021).

When we compared monitored with predicted soil loss, USLE predicted the same hierarchy of LULC as observed in the field monitoring. The long-term predicted mean soil loss was slightly under the estimated one for bare soil (3.5%), while it was overestimated for sugarcane (26.7%), WC (102.0%), and pasture (121.3%) covered plots. Nonetheless, the BIAS between observed and predicted soil loss was mostly systematic (Figure 5), which led to a high linear correlation between these two variables that can be used to correct the USLE estimations at other sites under same LULC. USLE predictions for BS plot had the highest performance ($R^2 = 0.85$) followed by PS ($R^2 = 0.80$), WC ($R^2 = 0.74$), and SC ($R^2 = 0.73$). Note that agricultural plots had a slight decay in model performance compared to the other ones, mostly due to soil management practices.

3.3 | Climate Change Scenarios

3.3.1 | MFI and Rainfall Erosivity

Among the two fitted curves for MFI index and rainfall erosivity, the exponential function had the highest correlation ($R^2 = 0.76$), followed by linear ($R^2 = 0.73$), and lastly the logarithmic ($R^2 = 0.65$). Therefore, we suggest Equation (10) for rainfall erosivity estimation based on daily or monthly rainfall observations.

$$R = 123.67\mathrm{MFI}^{0.57} \tag{10}$$

where R is the annual rainfall erosivity (MJ mm ha^{-1} h^{-1} year^{-1}), MFI (mm) is computed based on Equation (6).

By employing the local MFI (Equation 10) to bias-corrected climate change model output, we obtained the erosivity for historical and projected periods for SSP2-4.5 and SSP5-8.5 scenarios, using the CRHEA local station data (Figure 6). Figure 7 shows the annual distribution of climate modeling results, while Figure 8 summarizes the distribution of erosivity in the different periods and scenarios analyzed, as well as enabling a comparison with local estimations and observations. The IAB station had 10-min data records that enabled direct erosivity estimations while erosivity for the CRHEA station and climate

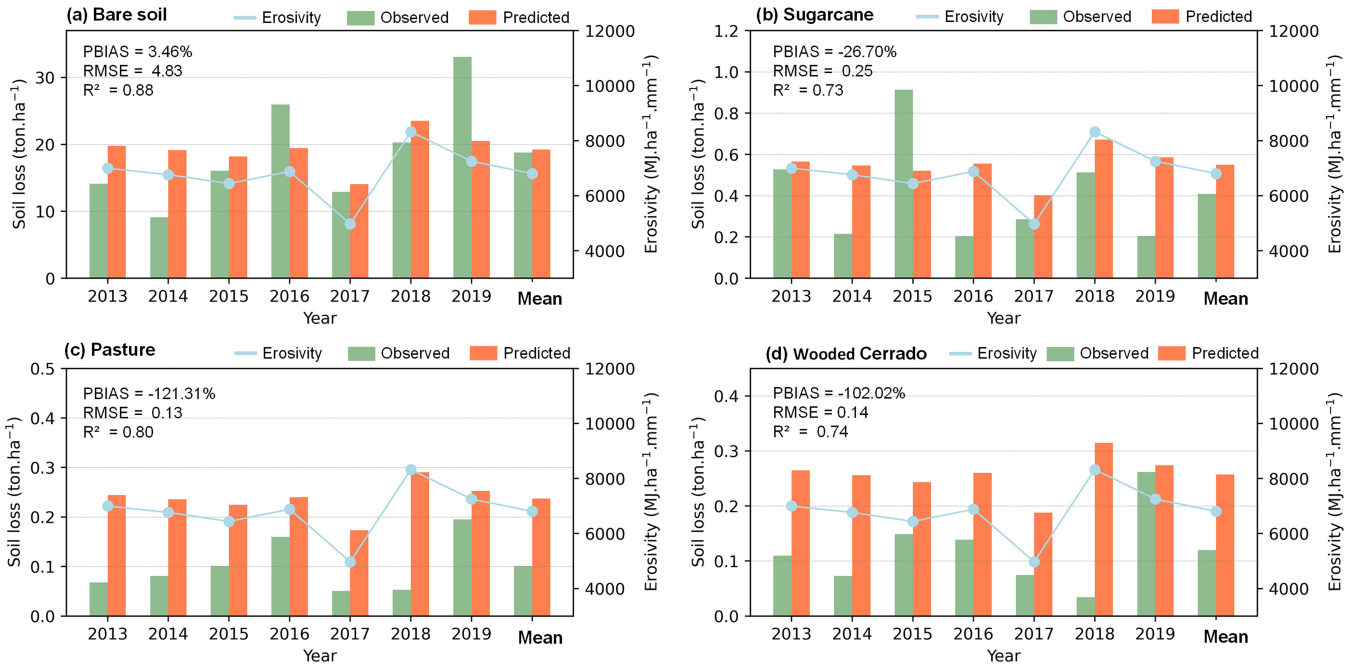

FIGURE 4 | Yearly monitored and estimated soil loss by USLE at bare soil (Figure 3a), sugarcane (Figure 3b), pasture (Figure 3c), and WC (Figure 3d). Aside from the points at yearly distribution is given the linear fitting curve and its associated coefficient of determination to each land cover. [Colour figure can be viewed at wileyonlinelibrary.com]

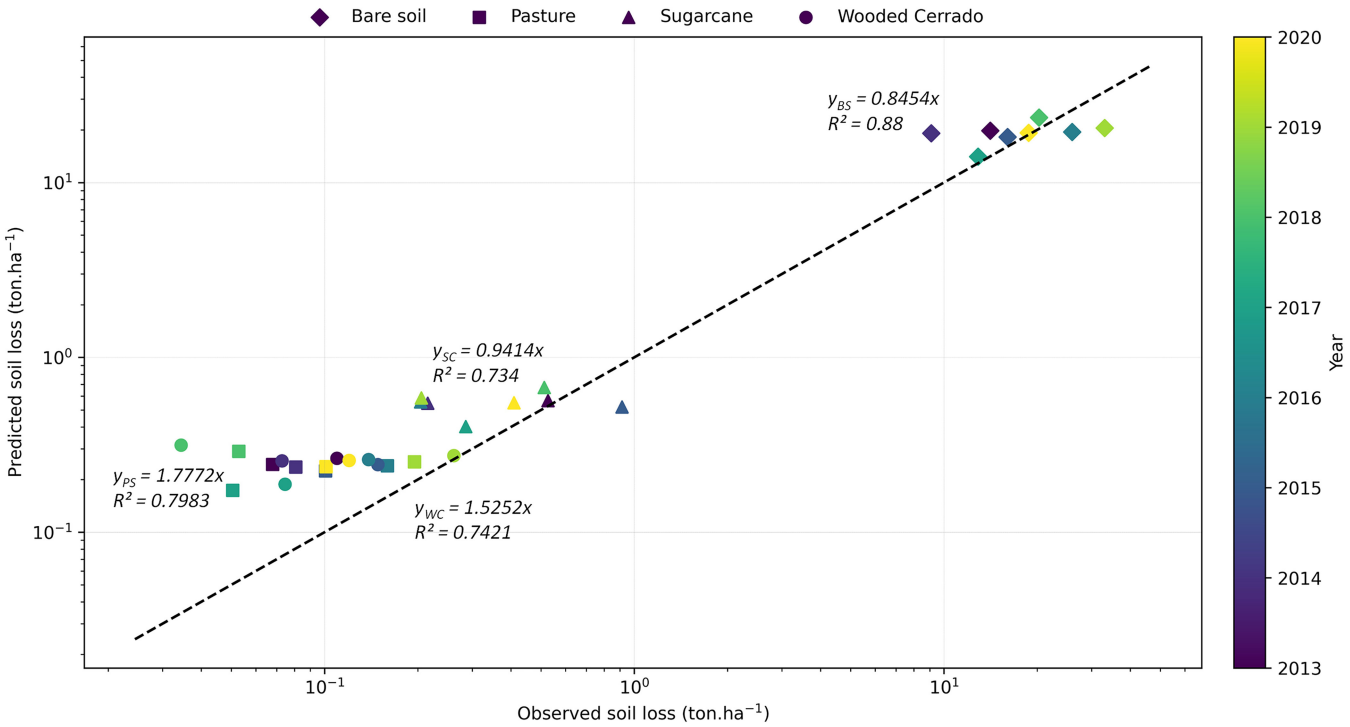

FIGURE 5 | Scatter of monitored and predicted soil loss (ton ha^{-1} year^{-1}) for the land cover analyzed. [Colour figure can be viewed at wileyonlinelibrary.com]

scenarios was estimated based on Equation (10). Among the reasons for the mismatch of erosivity between the CRHEA and IAB stations, first, the stations have different observation periods and second, the fitting curve failed to adjust to events of high intensity. On the other hand, the historical erosivity from the CRHEA monitoring station was within the range of estimated erosivity derived from climate models during the historical period and had similar distribution (p-value 0.05). This demonstrates the accordance with the climate model selection process and the validity of models in predictions for the projection period. In the intermediate future period, both SSP2-4.5 (mean of 6194 MJ mm ha^{-1} h^{-1} year^{-1} and model variation from 4627

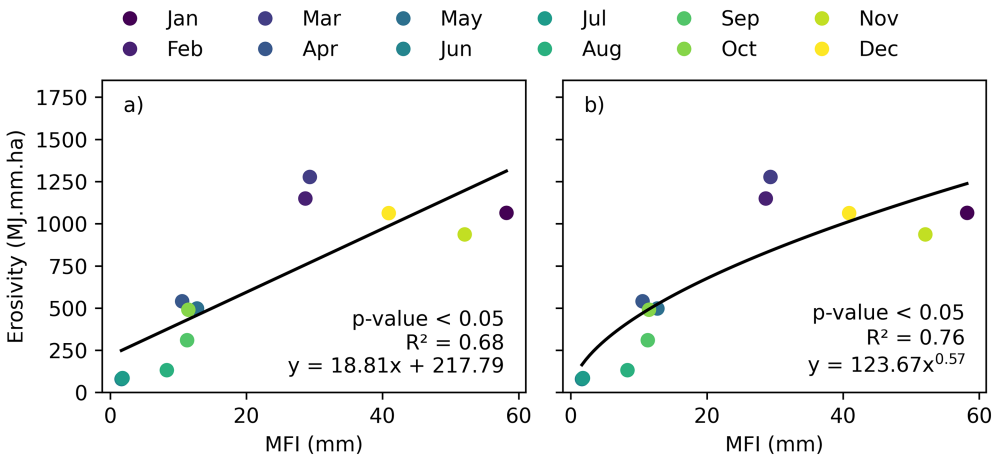

FIGURE 6 | Linear (a) and exponential (b) relationships between erosivity and MFI index for a monthly time step. [Colour figure can be viewed at wileyonlinelibrary.com]

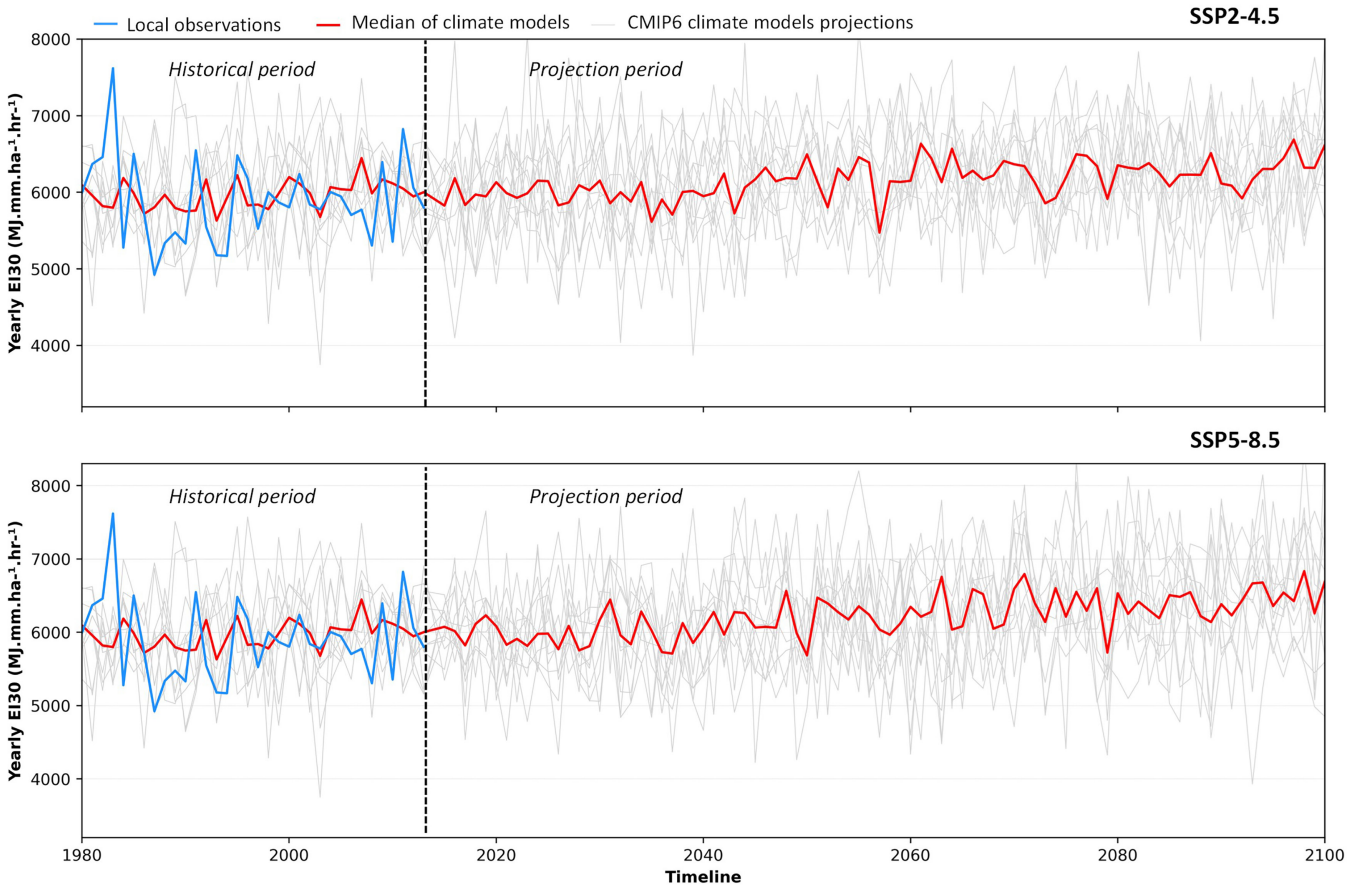

FIGURE 7 | Annual rainfall erosivity (MJ mm ha^{-1} h^{-1}) from individual CMIP6 climate projection models and field observations. [Colour figure can be viewed at wileyonlinelibrary.com]

to 8116) and SSP5-8.5 (mean of 6196 MJ mm ha^{-1} h^{-1} year^{-1} and model variation from 4624 to 8201) projected similar erosivity, representing a 3.8% rise as compared with the baseline period of 5891 MJ mm ha^{-1} h^{-1} year^{-1} (individual models ranging from 4923 to 7618). Looking toward the distant future, the mean EI30 showed a tendency to increase by 5% (individual models ranging from −34.1% to 43.7%) based on SSP2-4.5 scenario, reaching 6262 MJ mm ha^{-1} h^{-1} year^{-1} (individual models ranged from 4060 to 8004) compared to the baseline period. This effect was more prominent in the projections of the SSP5-8.5 (higher emissions scenario), as it exhibited the most pronounced growth rate in erosivity through the years reaching 6418 MJ mm ha^{-1} h^{-1} year^{-1} (individual models ranged from 3931 to 8575) until the end of the century.

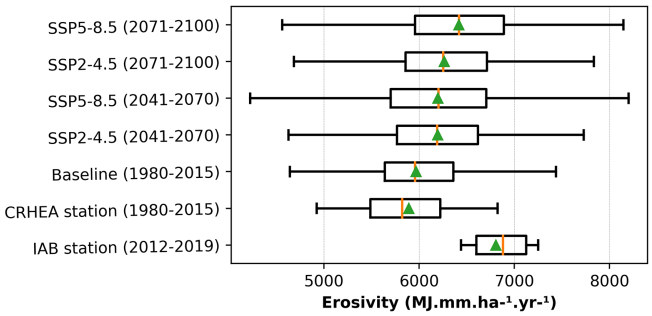

FIGURE 8 | Boxplots of annual erosivity based on local observations and climate change models for baseline and future time projections. Orange line indicates median, while green triangle indicates means. [Colour figure can be viewed at wileyonlinelibrary.com]

3.3.2 | Soil Loss Under Climate Change Projections

Complementing the analysis, from Figure 7 we note that the climate models included annual oscillations and therefore, analyzing individual annual erosivity would be inconsistent. Thus, we computed soil loss over two periods based on 30-year mean erosivity: intermediate future (2041–2070) and distant future (2071–2100) based on CMIP6 SSP2-4.5 and SSP5-8.5 climate projections compared with mean values during the baseline period for climate models, summarized in Table 4. In both scenarios, the increase in soil loss due to increasing rainfall erosivity is note-worthy. This effect is even more prominent in SSP5-8.5, which considers a higher anthropogenic interference on environment, especially in the distant future. In the intermediate future period (2040–2070), both SSP2-4.5 and SSP5-8.5 scenarios projected an increase of 3.8% and 3.9%, respectively. Looking forward to the distant future (2070–2100), the SSP2-4.5 path is projected to increase soil loss by 5%, while SSP5-8.5 scenario predicted a significant rising soil loss by about 8%.

4 | Discussion

The Brazilian WC is a major biome supporting agriculture that provides food for the entire world. One of the threats, however, is soil loss. In this study, we employed a unique database including 7 years of soil loss observations with experimental plots covering typical land uses (sugarcane, pasture, bare soil, and WC). The USLE model parameters were calibrated with high statistical correlation (R^2 ranging between 0.73 and 0.88) between observations and simulations. We employed the USLE parameters to estimate the soil loss rates under two climate change scenarios and the results indicated an increase of 4.9% (SSP2-4.5) and 7.6% (SSP5-8.5) in soil loss for all evaluated land covers until the end of the century compared with the baseline period. The calibrated USLE model is a simple but useful tool for soil loss estimation and the C and K factors can be employed for estimations in other not monitored areas. Similarly, they can also be employed to shed light on the still uncertain scene of climate change effects.

The subtropical climate C-factor identification for common agricultural and natural land cover (Table 5) serves as a foundation for a conservation-oriented framework and various investigations about the modeling of erosion and conservation of agricultural practices and land cover changes. Furthermore, it can facilitate soil loss rate estimations for areas that are not monitored, as well as enable projection of future trends in soil loss rates due to climate change (Table 4). Finally, the C-factors work as pivotal yardstick for gauging ecological actions, serving as a pertinent indicator for agro-environmental assessment (Prasuhn 2022). By drawing parallels from our local findings with previous investigations (Table 5), the *C*-values of crop sequence systems and natural forest in our research area were in the range of those found in other studies, except for sugarcane. This discrepancy can be attributed to the well-structured cropping system, which employed minimum soil disturbance, and fast-plant development with high leaf-index due to light, water, and nutrient abundance within our study area. There remains a limited body of Brazilian studies addressing the C factor (Cassol et al. 2018; Silva, Nachtigall, et al. 2020; Silva, Cassol, et al. 2020), while most of them are based on indirect estimations (e.g., NDVI) or short temporal observations (up to 2 years), our observations stand out as a unique subtropical seven-years data set.

Similar to the *R* calculations, there are many different ways in which erodibility can be calculated, based on textural information and organic matter (Renard et al. 1997; Wischmeier and Smith 1978), or estimated from a wide range of soil textures (Dymond 2010). Besides calculations, there are also large-scale erodibility data sets, such as for European (Panagos et al. 2014) and Brazilian territories (Godoi et al. 2021). Nevertheless, the values presented in large-scale data sets may not represent the local soil composition and therefore may lead to under- or over-estimation in soil loss by the USLE family equations. In Table 6 we summarize K-factors estimated for the Neossolo soil class in other study areas in Brazil and we note that there is a wide range of values. Among reasons, this may be mainly due to the different methodologies employed and the soil local composition (organic matter content and compaction level).

Soil loss rates at a monthly time scale from uncovered areas are highly dependent on rainfall erosivity, while smaller dependence is noted for covered plots (Figure 6). During the rainy season, the greatest losses occur not only due to more intense rainfall but also because consecutive rainfall events lead to higher soil saturation and consequently, greater runoff generation. Erosivity was calculated based on an empirical function with a varying rainfall intensity pattern and it is expected that this is not the complete driver of erosion in real environments. While interrill erosion is dominated by splash detachment (function of rainfall intensity), rill and gully erosion is dominated by runoff rate (not dependent of rainfall intensity) (Nearing et al. 2017; Cardoso et al. 2020). Our erosivity estimations are aligned with other erosivity estimations set in a global (Panagos et al. 2017; Liu et al. 2020), continental (Riquetti et al. 2020), national (Mello et al. 2013; Oliveira, Wendland, and Nearing 2013; Teixeira, Cecílio, Moreira, et al. 2022), and state perspective (Teixeira, Cecílio, Oliveira, et al. 2022). However, many previous studies have provided low spatial resolutions and/or based their estimations on indirect measurement methods. Besides employing local observations, we also correlated erosivity with the MFI index (Figure 6) to propose a relationship that enables

TABLE 4 | Estimated annual soil loss (ton ha^{-1} year^{-1}) based on CMIP6 SSP2-4.5 and SSP5-8.5 climate projections and USLE model. Each cell contains the variable value indicated on the top column accompanied by the standard deviation (after the sign ±).

Scenario	Period	Rainfall	Erosivity	Cerrado	Pasture	Sugarcane	Bare soil	Expected change[a]
Monitored	2012–2019	1330 ± 176	6804 ± 1002	0.120 ± 0.071	0.101 ± 0.056	0.409 ± 0.260	18.788 ± 8.312	—
Baseline	1980–2013	1503 ± 85	5966 ± 571	0.226 ± 0.022	0.208 ± 0.020	0.482 ± 0.046	16.861 ± 1.610	—
SSP2-4.5	2041–2070	1559 ± 81	6193 ± 625	0.234 ± 0.023	0.216 ± 0.022	0.500 ± 0.051	17.504 ± 1.769	3.82%
	2071–2100	1595 ± 75	6261 ± 635	0.236 ± 0.024	0.219 ± 0.022	0.506 ± 0.051	17.696 ± 1.795	4.95%
SSP5-8.5	2041–2070	1558 ± 82	6196 ± 718	0.234 ± 0.027	0.216 ± 0.025	0.500 ± 0.058	17.511 ± 2.032	3.86%
	2071–2100	1676 ± 102	6417 ± 758	0.243 ± 0.029	0.224 ± 0.026	0.519 ± 0.061	18.138 ± 2.144	7.57%

[a]Value based on the ratio between mean soil loss between projected and baseline periods of climate models.

further local erosivity estimation based on simple monthly rainfall data (Equation 10). There are only a few developed regression relationships for erosivity valid for the State of São Paulo, Brazil (Lombardi Neto and Moldenhauer 1992; Roque, Carvalho, and Prado 2001; Moreira et al. 2006; Silva, Iori, and Silva 2009; Teixeira, Cecílio, Oliveira, et al. 2022) and they are often either too generic for the broader area or locally developed for different climatic zones. As regression curves are site-specific, they cannot be directly used in other regions. Reliable erosivity estimations should be employed using further erosion modeling that can enable the identification of erosive hotspots and implementation of conservation practices.

The field observations indicated a current high soil loss rate in the BS plots, followed by SC, WC, and PS plots (see Table 4). All plots though, had soil loss below mean rates estimated for the state of São Paulo, Brazil (30 ton ha^{-1} year^{-1}, Medeiros et al. 2016). However, BS plots had soil loss rates that surpass a sustainable erosion limit for the Neossolo soil class that ranges from 5.2 (de Oliveira Pereira et al. 2008) to 12 ton ha^{-1} year^{-1} (Bertoni and Lombardi Neto 2017). Besides, within expected ranges, historical mean soil loss from sugarcane plots were much higher than from forested areas (Figure 4). With soil particles, nutrients are carried away from agricultural areas leading to eutrophication in lakes while increasing the need for agricultural fertilizers (Zhang et al. 2021). Even though PS had lower losses than WC plots, it generated high runoff, which also led to environmental disturbance.

There was a good agreement between the long-term mean observed and predicted soil loss, especially for the bare soil (yearly match with $R^2 = 0.88$ and overall underestimation of 3.5%). The reduced predictability in vegetated plots is related to the seasonal variation of the litter floor and leaf area, imposing higher variability in measured soil loss (Oliveira, Nearing, and Wendland 2015; Anache et al. 2018). The proposed USLE factors (Table 6 and Table 5) can be applied for soil loss estimation in other regions with similar soil composition and LULCs, creating outcomes similar to Medeiros et al. (2016), Gomes et al. (2017), and Riquetti et al. (2022) identify critical areas prone to erosion in São Paulo State, Cerrado biome, and South America, respectively. Soil erosion maps are valuable tools for the development of public policies, indication of where investments should be allocated, and recommendation of implementation of conservation practices.

The erosive force of rainfall is considered the major driver of soil and nutrient losses worldwide (Riquetti et al. 2020; Panagos et al. 2022). Our analyses projected an increase in erosivity at the intermediate (3.8% at SPP2-4.5 and 3.9% SSP5-8.5) and distant future (4.9% at SPP2–4.5 and 7.6% SSP5–8.5) for both climatic scenarios. Global estimations indicate a rise in erosivity between 30% (RCP4.5) and 34% (RCP8.5) by 2070 depending on climate scenario (Panagos et al. 2022). Riquetti et al. (2020) found contrasting changes in erosivity in South America and projected a reduction of erosivity by 15% in the Araguaia basin (Central part of Brazil) by considering RCP8.5 scenario until the end of the century. Colman et al. (2019) employed RUSLE and MIROC5 (RCM from CMIP5) and estimated that soil loss will increase by 12% by 2050 in the Pantanal biome region (Brazil). On the other hand, Anache et al. (2018) employed the WEPP model and MarkSim DSSAT dataset (weather generator at global scale using 17 CMIP5 General

TABLE 5 | Comparison of land cover (*C*) factors with other studies with similar hydro-climatic characteristics in Brazil.

Land cover	*C*-factor	State/Country	Reference
Wooded Cerrado	0.0133	São Paulo/Brazil	Current study
	0.013	São Paulo/Brazil	Oliveira, Nearing, and Wendland (2015)
	0,042	Minas gerais/Brazil	da Silva (2014)
	0.014	Mato Grosso do Sul/Brazil	Almagro et al. (2019)
Pasture	0.0123	São Paulo/Brazil	Current study
	0.030	São Paulo/Brazil	Galdino et al. (2015)
	0.020	São Paulo/Brazil	Oliveira, Nearing, and Wendland (2015)
	0.025	Mato Grosso do Sul/Brazil	Almagro et al. (2019)
Sugarcane	0.0286	São Paulo/Brazil	Current study
	0.1308	São Paulo/Brazil	Corrêa et al. (2016)
	0.096	Minas gerais/Brazil	Ayer et al. (2015)
	0.306	São Paulo/Brazil	Weill (1999)

TABLE 6 | Comparison of erodibility (*K*) factors from other studies with similar hydro-climatic characteristics in Brazil.

K-value	State/Country	Reference
0.00278	São Paulo/Brazil	Current study
0.0034	Minas Gerais/Brazil	Thoma et al. (2022)
0.0292	Goiás/Brazil	Galdino et al. (2015)
0.0372	Rio Grande do Sul/Brazil	Silva, Nachtigall, et al. (2020) Silva, Cassol, et al. (2020)
0.0440	São Paulo/Brazil	Lima et al. (2016)
0.0720	Mato Grosso do Sul/Brazil	Anache et al. (2015)
0.1448	São Paulo/Brazil	Mannigel et al. (2002)

Circulation Models) and found a significant change in erosion up to 2090 for an experimental plot in the Brazilian Cerrado. The difference between the cited studies relies on many aspects, such as spatial heterogeneity of climate change projections, the number of models employed, and their generation (Panagos et al. 2022). Our mean estimations are lower compared with other studies, but inside the range (minimum of −34.1% and a maximum of 43.7% at SSP5-8.5 for the period 2071–2100, see Table 4 and Figure 8). Here, we assembled 12 CMIP6 models, meaning that our findings are not heavily influenced by the bias of a singular model, but instead based on the consensus of multiple mathematical and physical approaches of these 12 models.

Besides the long-term predicted alteration of soil loss to the end of the century, we highlight that current land cover changes pose a bigger threat to soil conservation than climate change. The mean historical soil loss from sugarcane plots was 3.4 times higher than for pasture, while forest was 4.2 times smaller than the mean from agricultural areas (Figure 4). Current global land use change trends are characterized by increasing agricultural land cover over forested areas (Winkler et al. 2021). Actually, the Amazon biome has already lost 18% (Silveira et al. 2022) of its natural cover while the Cerrado has lost 53% (Beuchle et al. 2015) due to deforestation. These changes are estimated to correspond to up to 40% change in the atmospheric water budget (Wongchuig et al. 2023). The water flux over South America is intrinsically coupled to the Amazon where a massive air moisture strip, known as the South Atlantic Convergence Zone (SACZ). This commonly brings heavy rain from the north to the east of the continent (more than 2500 km long and 600 km wide), bringing the main source of tropospheric moisture to the South and Southeast Cerrado biome (Bergier et al. 2018; Colman et al. 2019). Alterations of rainfall patterns due to climate change may lead to changes in rainfall erosivity, that will impact the soil loss potential. Therefore, land conversion poses threats to soil loss at local and continental scales.

There are some limitations regarding the applicability of our results, however. Regarding the climate change findings, they were only based on changes in rainfall erosivity while major changes in vegetation development (Adams et al. 2017), root system (Calleja-Cabrera et al. 2020), phenology (Cleland et al. 2007), biomass (Tietjen et al. 2017), and species distribution (Penuelas and Boada 2003) were not accounted for. As well, the use of simple conservation practices such as tillage might have a major potential to mitigate up to 90% of climate change impacts (Chapman et al. 2021; Eekhout and de Vente 2022). Due to the complexity of the variables involved, further studies need to be carried out to conclude on how alteration of vegetation cover and conservation practices in combination with climate change will affect current patterns of soil loss.

5 | Conclusion

Climate change is expected to pose a threat to sustainable development and soil conservation. In this paper, we forecasted a rise in potential soil loss at the intermediate (2040–2070) and distant future (2070–2100). During the intermediate future period (2040–2070), both the SSP2-4.5 and SSP5-8.5 climate scenarios foresaw a 3.8% increase in soil loss. Shifting our gaze to the distant future period (2070–2100), the SSP2-4.5 scenario anticipated a 4.9% increase in soil loss, while the SSP5-8.5 scenario predicted a substantial 7.6% surge in soil loss.

To estimate soil loss, factors linked to the USLE model (erosivity, erodibility, and land cover) were locally computed. The utilization of field data to calculate these factors is essential for assessing soil erosion forecasts and generating region-specific or ecosystem-specific data that can be integrated into soil erosion models. Besides the limitations (yearly estimations, empirical model, etc.), USLE is a reliable model that can be used to estimate soil loss in ungauged basins and prioritize sustainable investments in high erosive areas.

Lastly, despite the increase in soil loss due to climate change, we argue that soil conservation already deals with a major threat that is even more serious than climate change, land cover change. Based on local monitoring, the soil loss in agricultural areas is 4.2 times higher than forest, highlighting the influence that land cover plays on soil conservation since more than 53% of the Cerrado biome has already been converted to agricultural areas. Our results contribute to the formulation of tailored soil and water conservation strategies for various regions of the Cerrado biome, thereby reducing the effects of soil erosion and promoting sustainable land-use practices.

Acknowledgments

The authors acknowledge the Graduate Program in Hydraulic Engineering and Sanitation (PPGSHS), University of São Paulo (USP-EESC), Department of Building and Environmental Technology, Lund University, for the scientific support, and the Arruda Botelho Institute (IAB) for allowing the development of this study on its land.

Data Availability Statement

The data that support the findings of this study are openly available in A decade of soil loss and runoff monitoring at Brazilian exp at https://zenodo.org/doi/10.5281/zenodo.10009738.

References

Adams, H. D., M. J. B. Zeppel, W. R. L. Anderegg, et al. 2017. "A Multi-Species Synthesis of Physiological Mechanisms in Drought-Induced Tree Mortality." *Nature Ecology & Evolution* 1, no. 9: 1285–1291. https://doi.org/10.1038/s41559-017-0248-x.

Aghsaei, H., N. Mobarghaee Dinan, A. Moridi, et al. 2020. "Effects of Dynamic Land Use/Land Cover Change on Water Resources and Sediment Yield in the Anzali Wetland Catchment, Gilan, Iran." *Science of the Total Environment* 712: 136449. https://doi.org/10.1016/j.scitotenv.2019.136449.

Almagro, A., P. T. S. Oliveira, M. A. Nearing, and S. Hagemann. 2017. "Projected Climate Change Impacts in Rainfall Erosivity Over Brazil." *Scientific Reports* 7, no. 1: 8130. https://doi.org/10.1038/s41598-017-08298-y.

Almagro, A., T. C. Thomé, C. B. Colman, et al. 2019. "Improving Cover and Management Factor (C-Factor) Estimation Using Remote Sensing Approaches for Tropical Regions." *International Soil and Water Conservation Research* 7, no. 4: 325–334. https://doi.org/10.1016/j.iswcr.2019.08.005.

Alvares, C. A., J. L. Stape, P. C. Sentelhas, J. L. de Moraes Gonc¸alves, and G. Sparovek. 2013. "Köppen's Climate Classification Map for Brazil." *Meteorologische Zeitschrift* 22, no. 6: 711–728. https://doi.org/10.1127/0941-2948/2013/0507.

Amanambu, A. C., L. Li, C. N. Egbinola, O. A. Obarein, C. Mupenzi, and D. Chen. 2019. "Spatio-Temporal Variation in Rainfall-Runoff Erosivity due to Climate Change in the Lower Niger Basin, West Africa." *Catena* 172: 324–334. https://doi.org/10.1016/j.catena.2018.09.003.

Anache, J. A., D. C. Flanagan, A. Srivastava, and E. C. Wendland. 2018. "Land Use and Climate Change Impacts on Runoff and Soil Erosion at the Hillslope Scale in the Brazilian Cerrado." *Science of the Total Environment* 622-623: 140–151. https://doi.org/10.1016/j.scitotenv.2017.11.257.

Anache, J. A. A., C. G. V. Bacchi, E. Panachuki, and T. Alves Sobrinho. 2015. "Assement of Methods for Predicting Soil Erodibility in Soil Modeling." *Geociências* 34, no. 1: 32–40.

Anache, J. A. A., E. Wendland, L. M. P. Rosalem, C. Youlton, and P. T. S. Oliveira. 2019. "Hydrological Trade-Offs due to Different Land Covers and Land Uses in the Brazilian Cerrado." *Hydrology and Earth System Sciences* 23, no. 3: 1263–1279. https://doi.org/10.5194/hess-23-1263-2019.

Arnoldus, H. M. J. 1977. "Methodology Used to Determine the Maximum Potential Range Average Annual Soil Loss to Sheet and Rill Erosion in Morocco." *Assessing Soil Degradation, FAO Soils Bulletin (FAO)* 34: 39–48.

Aslan, Z., G. Erdemir, E. Feoli, F. Giorgi, and D. Okcu. 2019. "Effects of Climate Change on Soil Erosion Risk Assessed by Clustering and Artificial Neural Network." *Pure and Applied Geophysics* 176, no. 2: 937–949. https://doi.org/10.1007/s00024-018-2010-y.

Atoma, H., K. V. Suryabhagavan, and M. Balakrishnan. 2020. "Soil Erosion Assessment Using RUSLE Model and GIS in Huluka Watershed, Central Ethiopia." *Sustainable Water Resources Management* 6, no. 1: 12. https://doi.org/10.1007/s40899-020-00365-z.

Ayer, J. E. B., D. Olivetti, R. L. Mincato, and M. L. N. Silva. 2015. "EroSão h'ıdrica em Latossolos Vermelhos distróficos." *Pesquisa Agropecuária Tropical* 45, no. 2: 180–191. https://doi.org/10.1590/1983-40632015v4531197.

Azari, M., A. Oliaye, and M. A. Nearing. 2021. "Expected Climate Change Impacts on Rainfall Erosivity Over Iran Based on CMIP5 Climate Models." *Journal of Hydrology* 593: 125826. https://doi.org/10.1016/j.jhydrol.2020.125826.

Bagarello, V., G. V. Di Piazza, V. Ferro, and G. Giordano. 2008. "Predicting Unit Plot Soil Loss in Sicily, South Italy." *Hydrological Processes* 22, no. 5: 586–595. https://doi.org/10.1002/hyp.6621.

Bagarello, V., V. Ferro, and D. Flanagan. 2018. "Predicting Plot Soil Loss by Empirical and Process-Oriented Approaches." *Journal of Agricultural Engineering* 49, no. 1: 1–18. https://doi.org/10.4081/jae.2018.710.

Bagarello, V., V. Ferro, and V. Pampalone. 2015. "Testing Assumptions and Procedures to Empirically Predict Bare Plot Soil Loss in a Mediterranean Environment." *Hydrological Processes* 29, no. 10: 2414–2424. https://doi.org/10.1002/hyp.10382.

Ballarin, A. S., J. S. Sone, G. C. Gesualdo, et al. 2023. "CLIMBra-Climate Change Dataset for Brazil." *Scientific Data* 10, no. 1: 47. https://doi.org/10.1038/s41597-023-01956-z.

Bergier, I., M. L. Assine, M. M. McGlue, et al. 2018. "Amazon Rainforest Modulation of Water Security in the Pantanal Wetland." *Science of the Total Environment* 619-620: 1116–1125. https://doi.org/10.1016/j.scitotenv.2017.11.163.

Bertoni, J., and F. Lombardi Neto. 2017. *Convervacão do Solo [Soil Conservation]*. 10th ed. Jaboticabal, São Paulo: Ícone.

Beuchle, R., R. C. Grecchi, Y. E. Shimabukuro, et al. 2015. "Land Cover Changes in the Brazilian Cerrado and Caatinga Biomes From 1990 to 2010 Based on a Systematic Remote Sensing Sampling Approach." *Applied Geography* 58: 116–127. https://doi.org/10.1016/j.apgeog.2015.01.017.

Bi, D., M. Dix, S. Marsland, et al. 2020. "Configuration and Spin-Up of ACCESS-CM2, the New Generation Australian Community Climate and Earth System Simulator Coupled Model." *Journal of Southern Hemisphere Earth Systems Science* 70, no. 1: 225–251. https://doi.org/10.1071/ES19040.

Biasutti, M., and R. Seager. 2015. "Projected Changes in US Rainfall Erosivity." *Hydrology and Earth System Sciences* 19, no. 6: 2945–2961. https://doi.org/10.5194/hess-19-2945-2015.

Bing, D., and S. Lei. 2022. "Remote Sensing Quantitative Research on Soil Erosion in the Upper Reaches of the Minjiang River." *Frontiers in Earth Science* 10: 930535. https://doi.org/10.3389/feart.2022.930535.

Bloschl, G., M. F. Bierkens, A. Chambel, et al. 2019. "Twenty-Three Unsolved Problems in Hydrology (UPH)—a Community Perspective." *Hydrological Sciences Journal* 64, no. 10: 1141–1158. https://doi.org/10.1080/02626667.2019.1620507.

Boardman, J. 2006. "Soil Erosion Science: Reflections on the Limitations of Current Approaches." *Catena* 68, no. 2–3: 73–86. https://doi.org/10.1016/j.catena.2006.03.007.

Bracken, L. J., and J. Croke. 2007. "The Concept of Hydrological Connectivity and Its Contribution to Understanding Runoff- Dominated Geomorphic Systems." *Hydrological Processes* 21, no. 13: 1749–1763. https://doi.org/10.1002/hyp.6313.

Brown, L. C., and G. R. Foster. 1987. "Storm Erosivity Using Idealized Intensity Distributions." *Transactions of ASAE* 30, no. 2: 379–386. https://doi.org/10.13031/2013.31957.

Calleja-Cabrera, J., M. Boter, L. Oñate-Sa'nchez, and M. Pernas. 2020. "Root Growth Adaptation to Climate Change in Crops." *Frontiers in Plant Science* 11: 544. https://doi.org/10.3389/fpls.2020.00544.

Cao, J., B. Wang, Y.-M. Yang, et al. 2018. "The NUIST Earth System Model (NESM) Version 3: Description and Preliminary Evaluation." *Geoscientific Model Development* 11, no. 7: 2975–2993. https://doi.org/10.5194/gmd-11-2975-2018.

Cardoso, D. P., E. M. Silva, J. C. Avanzi, et al. 2020. "RainfallErosivityFactor: An R Package for Rainfall Erosivity (R-Factor) Determination." *Catena* 189: 104509. https://doi.org/10.1016/j.catena.2020.104509.

Cassol, E. A., T. S. D. Silva, F. L. F. Eltz, and R. Levien. 2018. "Soil Erodibility Under Natural Rainfall Conditions as the K Factor of the Universal Soil Loss Equation and Application of the Nomograph for a Subtropical Ultisol." *Revista Brasileira de Ciência do Solo* 42: e0170262. https://doi.org/10.1590/18069657rbcs20170262.

Chalise, D., L. Kumar, R. Sharma, and P. Kristiansen. 2020. "Assessing the Impacts of Tillage and Mulch on Soil Erosion and Corn Yield." *Agronomy* 10, no. 1: 63. https://doi.org/10.3390/agronomy10010063.

Chapman, S., C. E. Birch, M. V. Galdos, et al. 2021. "Assessing the Impact of Climate Change on Soil Erosion in East Africa Using a Convection-Permitting Climate Model." *Environmental Research Letters* 16, no. 8: 084006. https://doi.org/10.1088/1748-9326/ac10e1.

Cima, I. S., S. Amaral, and K. G. Massi. 2023. "Mapping Cerrado Remnants in an Anthropized Landscape in Southeast Brazil." *Remote Sensing Applications: Society and Environment* 32: 101032. https://doi.org/10.1016/j.rsase.2023.101032.

Cleland, E., I. Chuine, A. Menzel, H. Mooney, and M. Schwartz. 2007. "Shifting Plant Phenology in Response to Global Change." *Trends in Ecology & Evolution* 22, no. 7: 357–365. https://doi.org/10.1016/j.tree.2007.04.003.

Colman, C. B., P. T. S. Oliveira, A. Almagro, B. S. Soares-Filho, and D. B. Rodrigues. 2019. "Effects of Climate and Land-Cover Changes on Soil Erosion in Brazilian Pantanal." *Sustainability* 11, no. 24: 1–16. https://doi.org/10.3390/su11247053.

Corrêa, E. A., I. C. Moraes, S. d. A. F. Pinto, and C. M. Lupinacci. 2016. "Soil Losses, Soil Loss Ratio and Cover Management Factor of Sugarcane: A First Approach." *Revista do Departamento de Geografia* 32: 72–87.

Costa Junior, C., M. d. C. Píccolo, M. Siqueira Neto, P. B. d. Camargo, C. C. Cerri, and M. Bernoux. 2012. "Carbono em agregados do solo sob vegetação nativa, pastagem e sistemas agrícolas no bioma Cerrado." *Revista Brasileira de Ciência do Solo* 36, no. 4: 1311–1322. https://doi.org/10.1590/S0100-06832012000400025.

da Silva, V. C. 2014. "Estimativa da eroSão atual da bacia do Rio Paracatu (MG, GO, DF)." *Pesquisa Agropecuária Tropical* 34, no. 3: 147–159.

Dawadi, S., and S. Ahmad. 2013. "Evaluating the Impact of Demand-Side Management on Water Resources Under Changing Climatic Conditions and Increasing Population." *Journal of Environmental Management* 114: 261–275. https://doi.org/10.1016/j.jenvman.2012.10.015.

de Oliveira Pereira, F., D. Santos, I. da Silva de França, and M. L. Silva Naves. 2008. "Tolerância de Perda de Solo por Erosão para o Estado da Paraíba." *Revista de Biologia e Ciências da Terra* 8, no. 2: 60–71.

Doscher, R., M. Acosta, A. Alessandri, et al. 2022. "The EC-Earth3 Earth System Model for the Coupled Model Intercomparison Project 6." *Geoscientific Model Development* 15, no. 7: 2973–3020. https://doi.org/10.5194/gmd-15-2973-2022.

Dunne, J. P., L. W. Horowitz, A. J. Adcroft, et al. 2020. "The GFDL Earth System Model Version 4.1 (GFDL-ESM 4.1): Overall Coupled Model Description and Simulation Characteristics." *Journal of Advances in Modeling Earth Systems* 12: e2019MS002015. https://doi.org/10.1029/2019MS002015.

Duulatov, E., X. Chen, A. C. Amanambu, et al. 2019. "Projected Rainfall Erosivity Over Central Asia Based on CMIP5 Climate Models." *Water* 11, no. 5: 897. https://doi.org/10.3390/w11050897.

Dymond, J. R. 2010. "Soil Erosion in New Zealand Is a Net Sink of CO2." *Earth Surface Processes and Landforms* 35, no. 15: 1763–1772. https://doi.org/10.1002/esp.2014.

Eekhout, J. P., and J. de Vente. 2022. "Global Impact of Climate Change on Soil Erosion and Potential for Adaptation Through Soil Conservation." *Earth-Science Reviews* 226: 103921. https://doi.org/10.1016/j.earscirev.2022.103921.

EMBRAPA EBDPA. 1997. *Manual de me'todos de ana'lise de solos* (tech. rep.). Rio de Janeiro, RJ: Centro Nacional de Pesquisa de Solo.

Galdino, S., E. E. Sano, R. G. Andrade, et al. 2015. "Large-Scale Modeling of Soil Erosion With RUSLE for Conservationist Planning of Degraded Cultivated Brazilian Pastures." *Land Degradation & Development* 27, no. 3: 773–784. https://doi.org/10.1002/ldr.2414.

Ghosal, K., and S. Das Bhattacharya. 2020. "A Review of RUSLE Model." *Journal of the Indian Society of Remote Sensing* 48, no. 4: 689–707. https://doi.org/10.1007/s12524-019-01097-0.

Godoi, R. d. F., D. B. Rodrigues, P. Borrelli, and P. T. S. Oliveira. 2021. "High-Resolution Soil Erodibility Map of Brazil." *Science of the Total Environment* 781: 146673. https://doi.org/10.1016/j.scitotenv.2021.146673.

Gomes, L., S. J. C. Simões, M. C. Forti, J. P. H. B. Ometto, and E. L. D. Nora. 2017. "Using Geotechnology to Estimate Annual Soil Loss Rate in the Brazilian Cerrado." *Journal of Geographic Information System* 09, no. 4: 420–439. https://doi.org/10.4236/jgis.2017.94026.

Gutjahr, O., D. Putrasahan, K. Lohmann, et al. 2019. "Max Planck Institute Earth System Model (MPI-ESM1.2) for the High-Resolution Model Inter- Comparison Project (HighResMIP)." *Geoscientific Model Development* 12, no. 7: 3241–3281. https://doi.org/10.5194/gmd-12-3241-2019.

Hailu, A., S. Mammo, and M. Kidane. 2020. "Dynamics of Land Use, Land Cover Change Trend and Its Drivers in Jimma Geneti District, Western Ethiopia." *Land Use Policy* 99: 105011. https://doi.org/10.1016/j.landusepol.2020.105011.

Hateffard, F., S. Mohammed, K. Alsafadi, et al. 2021. "CMIP5 Climate Projections and RUSLE-Based Soil Erosion Assessment in the Central Part of Iran." *Scientific Reports* 11, no. 1: 1–17. https://doi.org/10.1038/s41598-021-86618-z.

Held, I. M., H. Guo, A. Adcroft, et al. 2019. "Structure and Performance of GFDL's CM4.0 Climate Model." *Journal of Advances in Modeling Earth Systems* 11, no. 11: 3691–3727. https://doi.org/10.1029/2019MS001829.

Hou, X., J. Shao, X. Chen, J. Li, and J. Lu. 2020. "Changes in the Soil Erosion Status in the Middle and Lower Reaches of the Yangtze River Basin From 2001 to 2014 and the Impacts of Erosion on the Water Quality of Lakes and Reservoirs." *International Journal of Remote Sensing* 41, no. 8: 3175–3196. https://doi.org/10.1080/01431161.2019.1699974.

Kinnell, P. I. A., and L. M. Risse. 1998. "USLE-M: Empirical Modeling Rainfall Erosion Through Runoff and Sediment Concentration." *Soil Science Society of America Journal* 62, no. 6: 1667–1672. https://doi.org/10.2136/sssaj1998.03615995006200060026x.

Lal, M., S. K. Mishra, A. Pandey, et al. 2017. "Evaluation of the Soil Conservation Service Curve Number Methodology Using Data From Agricultural Plots." *Hydrogeology Journal* 25, no. 1: 151–167. https://doi.org/10.1007/s10040-016-1460-5.

Law, R. M., T. Ziehn, R. J. Matear, et al. 2017. "The Carbon Cycle in the Australian Community Climate and Earth System Simulator (ACCESS-ESM1)—Part 1: Model Description and Pre-Industrial Simulation." *Geoscientific Model Development* 10, no. 7: 2567–2590. https://doi.org/10.5194/gmd-10-2567-2017.

Lee, J., J. Kim, M.-A. Sun, et al. 2020. "Evaluation of the Korea Meteorological Administration Advanced Community Earth-System Model (K-ACE)." *Asia-Pacific Journal of Atmospheric Sciences* 56, no. 3: 381–395. https://doi.org/10.1007/s13143-019-00144-7.

Lima, C. G. d. R., M. d. P. Carvalho, A. Souza, N. R. Costa, and R. Montanari. 2016. "Influence of Chemical Attributes in Erodibility and Tolerance of Soil Loss in Watershed of Low São Jose´ of Dourados River." *Geociencias* 35, no. 1: 63–76.

Liu, Y., W. Zhao, Y. Liu, and P. Pereira. 2020. "Global Rainfall Erosivity Changes Between 1980 and 2017 Based on an Erosivity Model Using Daily Precipitation Data." *Catena* 194: 104768. https://doi.org/10.1016/j.catena.2020.104768.

Lombardi Neto, F., and W. C. Moldenhauer. 1992. "Erosividade da chuva: sua distribuição e relação com as perdas de solo em Campinas (SP)." *Bragantia* 51, no. 2: 189–196. https://doi.org/10.1590/S0006-87051992000200009.

Mannigel, A. R., M. D. P. E Carvalho, D. Moreti, and L. D. R. Medeiros. 2002. "Fator erodibilidade e tolerância de perda dos solos do Estado de São Paulo." *Acta Scientiarum Agronomy* 24: 1335–1340. https://doi.org/10.4025/actasciagron.v24i0.2374.

McCool, D. K., L. C. Brown, G. R. Foster, C. K. Mutchler, and L. D. Meyer. 1987. "Revised Slope Steepness Factor for the Universal Soil Loss Equation." *Transactions of ASAE* 30, no. 5: 1387–1396. https://doi.org/10.13031/2013.30576.

Medeiros, G. D. O. R., A. Giarolla, G. Sampaio, and M. A. Marinho. 2016. "Estimates of Annual Soil Loss Rates in the State of São Paulo, Brazil." *Revista Brasileira de Ciência do Solo* 40: e0150497. https://doi.org/10.1590/18069657rbcs20150497.

Mello, C., M. Viola, S. Beskow, and L. Norton. 2013. "Multivariate Models for Annual Rainfall Erosivity in Brazil." *GeoDerma* 202-203: 88–102. https://doi.org/10.1016/j.geoderma.2013.03.009.

Mohammed, S., H. G. Abdo, S. Szabo, et al. 2020. "Estimating Human Impacts on Soil Erosion Considering Different Hillslope Inclinations and Land Uses in the Coastal Region of Syria." *Watermark* 12, no. 10: 2786. https://doi.org/10.3390/w12102786.

Mohammed, S., K. Alsafadi, S. Talukdar, et al. 2020. "Estimation of Soil Erosion Risk in Southern Part of Syria by Using RUSLE Integrating Geo Informatics Approach." *Remote Sensing Applications: Society and Environment* 20: 100375. https://doi.org/10.1016/j.rsase.2020.100375.

Molina-Sanchis, I., R. Lázaro, E. Arnau-Rosalén, and A. Calvo-Cases. 2016. "Rainfall Timing and Runoff: The Influence of the Criterion for Rain Event Separation." *Journal of Hydrology and Hydromechanics* 64, no. 3: 226–236. https://doi.org/10.1515/johh-2016-0024.

Moreira, M. C., R. A. Cecílio, F. d. A. d. C. Pinto, and F. F. Pruski. 2006. "Estimates of Rainfall Erosivity in São Paulo State by an Artificial Neural Network." *Revista Brasileira de Ciência do Solo* 30, no. 6: 1069–1076. https://doi.org/10.1590/S0100-06832006000600016.

Müller, W. A., J. H. Jungclaus, T. Mauritsen, et al. 2018. "A Higher-Resolution Version of the Max Planck Institute Earth System Model (MPI-ESM1.2-HR)." *Journal of Advances in Modeling Earth Systems* 10, no. 7: 1383–1413. https://doi.org/10.1029/2017MS001217.

Myers, N., R. A. Mittermeier, C. G. Mittermeier, G. A. B. da Fonseca, and J. Kent. 2000. "Biodiversity Hotspots for Conservation Priorities." *Nature* 403, no. 6772: 853–858. https://doi.org/10.1038/35002501.

Nacinovic, M. G. G., C. F. Mahler, and A. d. S. Avelar. 2014. "Soil Erosion as a Function of Different Agricultural Land Use in Rio de Janeiro." *Soil and Tillage Research* 144: 164–173. https://doi.org/10.1016/j.still.2014.07.002.

Nearing, M. A., S.-q. Yin, P. Borrelli, and V. O. Polyakov. 2017. "Rainfall Erosivity: An Historical Review." *Catena* 157: 357–362. https://doi.org/10.1016/j.catena.2017.06.004.

Nyesheja, E. M., X. Chen, A. M. El-Tantawi, F. Karamage, C. Mupenzi, and J. B. Nsengiyumva. 2019. "Soil Erosion Assessment Using RUSLE Model in The Congo Nile Ridge Region of Rwanda." *Physical Geography* 40, no. 4: 339–360. https://doi.org/10.1080/02723646.2018.1541706.

Oliveira, P. T. S., M. C. Lucas, R. de Faria Godoi, and E. Wendland. 2021. "Chapter 29-Groundwater Recharge and Sustainability in Brazil." In *Global Groundwater*, edited by A. Mukherjee, B. R. Scanlon, A. Aureli, S. Langan, H. Guo, and A. A. McKenzie, 393–407. São Carlos, São Paulo: Elsevier. https://doi.org/10.1016/B978-0-12-818172-0.00029-3.

Oliveira, P. T. S., M. A. Nearing, and E. Wendland. 2015. "Orders of Magnitude Increase in Soil Erosion Associated With Land Use Change From Native to Cultivated Vegetation in a Brazilian Savannah Environment." *Earth Surface Processes and Landforms* 40, no. 11: 1524–1532. https://doi.org/10.1002/esp.3738.

Oliveira, P. T. S., E. Wendland, and M. A. Nearing. 2013. "Rainfall Erosivity in Brazil: A Review." *Catena* 100: 139–147. https://doi.org/10.1016/j.catena.2012.08.006.

Oliveira, P. T. S., E. Wendland, M. A. Nearing, R. L. Scott, R. Rosolem, and H. R. da Rocha. 2015. "The Water Balance Components of Undisturbed Tropical Woodlands in the Brazilian Cerrado." *Hydrology and Earth System Sciences* 19, no. 6: 2899–2910. https://doi.org/10.5194/hess-19-2899-2015.

O'Neill, B. C., C. Tebaldi, D. P. van Vuuren, et al. 2016. "The Scenario Model Inter- Comparison Project (ScenarioMIP) for CMIP6." *Geoscientific Model Development* 9, no. 9: 3461–3482. https://doi.org/10.5194/gmd-9-3461-2016.

Panagos, P., P. Borrelli, F. Matthews, et al. 2022. "Global Rainfall Erosivity Projections for 2050 and 2070." *Journal of Hydrology* 610: 127865. https://doi.org/10.1016/j.jhydrol.2022.127865.

Panagos, P., P. Borrelli, K. Meusburger, et al. 2017. "Global Rainfall Erosivity Assessment Based on High-Temporal Resolution Rainfall Records." *Scientific Reports* 7, no. 1: 4175. https://doi.org/10.1038/s41598-017-04282-8.

Panagos, P., K. Meusburger, C. Ballabio, P. Borrelli, and C. Alewell. 2014. "Soil Erodibility in Europe: A High-Resolution Dataset Based on LUCAS." *Science of the Total Environment* 479-480: 189–200. https://doi.org/10.1016/j.scitotenv.2014.02.010.

Penuelas, J., and M. Boada. 2003. "A Global Change-Induced Biome Shift in the Montseny Mountains (NE Spain)." *Global Change Biology* 9, no. 2: 131–140. https://doi.org/10.1046/j.1365-2486.2003.00566.x.

Pham, T. G., J. Degener, and M. Kappas. 2018. "Integrated Universal Soil Loss Equation (USLE) and Geographical Information System (GIS) for Soil Erosion Estimation in A Sap Basin: Central Vietnam." *International Soil and Water Conservation Research* 6, no. 2: 99–110. https://doi.org/10.1016/j.iswcr.2018.01.001.

Prasuhn, V. 2022. "Experience With the Assessment of the USLE Cover-Management Factor for Arable Land Compared With Long-Term Measured Soil Loss in the Swiss Plateau." *Soil and Tillage Research* 215: 105199. https://doi.org/10.1016/j.still.2021.105199.

Prăvălie, R. 2021. "Exploring the Multiple Land Degradation Pathways Across the Planet." *Earth-Science Reviews* 220: 103689. https://doi.org/10.1016/j.earscirev.2021.103689.

Renard, K., G. Foster, G. Weesies, D. McCool, and D. Yoder. 1997. *Predicting Soil Erosion by Water: A Guide To Conservation Planning With The Revised Universal Soil Loss Equation (RUSLE)*. Washington: US Department of Agricultural Handbook.

Ribeiro, J. F., and B. M. T. Walter. 2008. "As Principais Fitofisionomias do Bioma Cerrado." In *Cerrado: ecologia e flora v. 2*, edited by S. M. Sano, S. P. d. Almeida, and J. F. Ribeiro, 876. Brasília: EMBRAPA-CERRADOS.

Riquetti, N. B., C. R. Mello, S. Beskow, and M. R. Viola. 2020. "Rainfall Erosivity in South America: Current Patterns and Future Perspectives." *Science of the Total Environment* 724: 138315. https://doi.org/10.1016/j.scitotenv.2020.138315.

Riquetti, N. B., C. R. Mello, D. Leandro, J. A. Guzman, and S. Beskow. 2022. "Assessment of the Soil-Erosion-Sediment for Sustainable Development of South America." *Journal of Environmental Management* 321: 115933. https://doi.org/10.1016/j.jenvman.2022.115933.

Rocha, G. C., and G. Sparovek. 2021. "Scientific and Technical Knowledge of Sugarcane Cover-Management USLE/RUSLE Factor." *Scientia Agricola* 78, no. suppl 1: e20200234. https://doi.org/10.1590/1678-992X-2020-0234.

Roque, C. G., M. P. Carvalho, and R. M. Prado. 2001. "Fator erosividade da chuva de Piraju (SP): distribuição, probabilidade de ocorrência, período de retorno e correlação com o coeficiente de chuva." *Revista Brasileira de Ciência do Solo* 25, no. 1: 147–156. https://doi.org/10.1590/S0100-06832001000100016.

Roy, P., S. C. Pal, R. Chakrabortty, A. Saha, and I. Chowdhuri. 2023. "A Systematic Review on Climate Change and Geo- Environmental Factors Induced Land Degradation: Processes, Policy-Practice Gap and Its Management Strategies." *Geological Journal* 58, no. 9: 3487–3514. https://doi.org/10.1002/gj.4649.

Santos, F. F. D. M., G. Durigan, R. S. Boschi, N. Ivanauskas, and R. R. Rodrigues. 2024. "Tree Community Dynamics in the cerradão (2002-2016): A Case of Biome Shift." *Forest Ecology and Management* 555: 121698. https://doi.org/10.1016/j.foreco.2024.121698.

Schwamback, D., A. R. Amorim Brandão, L. M. P. Rosalem, et al. 2024. "Land use transformations in the Brazilian Savanna: A decade of soil erosion and runoff measurements." *CATENA* 246: 108412. https://doi.org/10.1016/j.catena.2024.108412.

Sellar, A. A., C. G. Jones, J. P. Mulcahy, et al. 2019. "UKESM1: Description and Evaluation of the U.K. Earth System Model." *Journal of Advances in Modeling Earth Systems* 11, no. 12: 4513–4558. https://doi.org/10.1029/2019MS001739.

Silva, R. B., P. Iori, and F. A. M. Silva. 2009. "Proposition and Compare of Equations to Estimate the Rainfall Erosivity in Two Cities of São Paulo State." *Irriga* 14, no. 4: 533–547. https://doi.org/10.15809/irriga.2009v14n4p533-547.

Silva, T. P., S. D. Nachtigall, M. C. M. Nunes, C. L. R. Lima, and A. P. Knapp. 2020. "Modeling of Wate Erosion in a Sub-Basin in Rio Grande Do Sul Using RUSLE Model." *Revista Engenharia Na Agricultura - REVENG* 28: 302–313. https://doi.org/10.13083/reveng.v29i1.8930.

Silva, T. S. D., E. A. Cassol, R. Levien, F. L. F. Eltz, and M. R. Schmidt. 2020. "Long-Term Wheat-Soybean Successions Affecting the Cover and Soil Management Factor in USLE, Under Subtropical Climate." *Revista Brasileira de Ciência do Solo* 44: e0190180. https://doi.org/10.36783/18069657rbcs20190180.

Silveira, J. G. D., S. N. D. Oliveira Neto, A. C. B. D. Canto, et al. 2022. "Land Use, Land Cover Change and Sustainable Intensification of Agriculture and Livestock in the Amazon and the Atlantic Forest in Brazil." *Sustainability* 14, no. 5: 2563. https://doi.org/10.3390/su14052563.

Siqueira, P. P., P. T. S. Oliveira, D. Bressiani, A. A. Meira Neto, and D. B. Rodrigues. 2021. "Effects of Climate and Land Cover Changes on Water Availability in a Brazilian Cerrado Basin." *Journal of Hydrology: Regional Studies* 37: 100931. https://doi.org/10.1016/j.ejrh.2021.100931.

Souza, C. M., J. Z. Shimbo, M. R. Rosa, et al. 2020. "Reconstructing Three Decades of Land Use and Land Cover Changes in Brazilian Biomes With Landsat Archive and Earth Engine." *Remote Sensing* 12, no. 17: 2735. https://doi.org/10.3390/rs12172735.

Spera, S. 2017. "Agricultural Intensification Can Preserve the Brazilian Cerrado: Applying Lessons From Mato Grosso and Goia's to Brazil's Last Agricultural Frontier." *Tropical Conservation Science* 10: 194008291772066. https://doi.org/10.1177/1940082917720662.

Stabile, M. C., A. L. Guimarães, D. S. Silva, et al. 2020. "Solving Brazil's Land Use Puzzle: Increasing Production and Slowing Amazon Deforestation." *Land Use Policy* 91: 104362. https://doi.org/10.1016/j.landusepol.2019.104362.

Stefanidis, S., and D. Stathis. 2018. "Effect of Climate Change on Soil Erosion in a Mountainous Mediterranean Catchment (Central Pindus, Greece)." *Watermark* 10, no. 10: 1469. https://doi.org/10.3390/w10101469.

Strassburg, B. B. N., T. Brooks, R. Feltran-Barbieri, et al. 2017. "Moment of Truth for the Cerrado Hotspot." *Nature Ecology & Evolution* 1, no. 4: 0099. https://doi.org/10.1038/s41559-017-0099.

Tatebe, H., T. Ogura, T. Nitta, et al. 2019. "Description and Basic Evaluation of Simulated Mean State, Internal Variabil- Ity, and Climate Sensitivity in MIROC6." *Geoscientific Model Development* 12, no. 7: 2727–2765. https://doi.org/10.5194/gmd-12-2727-2019.

Tebaldi, C., K. Debeire, V. Eyring, et al. 2021. "Climate Model Projections From the Scenario Model Intercomparison Project (ScenarioMIP) of CMIP6." *Earth System Dynamics* 12, no. 1: 253–293. https://doi.org/10.5194/esd-12-253-2021.

Teixeira, D. B. d. S., R. A. Cecílio, M. C. Moreira, G. F. Pires, and E. I. Fernandes Filho. 2022. "Recent Advancements in Rainfall Erosivity

Assessment in Brazil: A Review." *Catena* 219: 106572. https://doi.org/10.1016/j.catena.2022.106572.

Teixeira, D. B. d. S., R. A. Cecílio, J. P. B. d. Oliveira, L. T. d. Almeida, and G. F. Pires. 2022. "Rainfall Erosivity and Erosivity Density Through Rainfall Synthetic Series for São Paulo State, Brazil: Assessment, Regionalization and Modeling." *International Soil and Water Conservation Research* 10, no. 3: 355–370. https://doi.org/10.1016/j.iswcr.2021.10.002.

Thoma, A. C., D. Tassinari, B. V. Prat, J. S. C. Fernandes, and A. C. Silva. 2022. "Erodibilidade de Neossolo Litólico pelo ensaio de Inderbitzen modificado e eficiência de blocos de solo-cimento para controle da erosão hídrica." *Engenharia Sanitaria e Ambiental* 27, no. 3: 511–522. https://doi.org/10.1590/s1413-415220210099.

Tietjen, B., D. R. Schlaepfer, J. B. Bradford, et al. 2017. "Climate Change-Induced Vegetation Shifts Lead to More Ecological Droughts Despite Projected Rainfall Increases in Many Global Temperate Drylands." *Global Change Biology* 23, no. 7: 2743–2754. https://doi.org/10.1111/gcb.13598.

Todisco, F., L. Vergni, F. Mannocchi, and C. Bomba. 2012. "Calibration of the Soil Loss Measurement Method at the Masse Experimental Station." *Catena* 91: 4–9. https://doi.org/10.1016/j.catena.2011.02.003.

Tu, A., J. Zeng, Z. Liu, H. Zheng, and S. Xie. 2023. "Effect of Minimum Inter-Event Time for Rainfall Event Separation on Rainfall Properties and Rainfall Erosivity in a Humid Area of Southern China." *Geoderma* 431: 116332. https://doi.org/10.1016/j.geoderma.2023.116332.

USDA. 2013. "Rainfall Intensity Summarization Tool (RIST)." https://www.ars.usda.gov/southeast-area/oxford-ms/national-sedimentation-laboratory/watershed-physical-processes-research/research/rist/rist-rainfall-intensity-summarization-tool/.

Valdes, C., K. Hjort, and R. Seeley. 2020. "*Brazil's Currency Depreciation and Changing Macroeconomic Conditions Determine Agricultural Competitiveness and Future Growth*." (tech. rep. No. 276). www.ers.usda.gov.

Veettil, A. V., and A. Mishra. 2020. "Water Security Assessment for the Contiguous United States Using Water Footprint Concepts." *Geophysical Research Letters* 47, no. 7: e2020GL087061. https://doi.org/10.1029/2020GL087061.

Vendrame, P. R., O. R. Brito, M. F. Guimarães, E.́. S. Martins, and T. Becquer. 2010. "Fertility and Acidity Status of Latossolos (Oxisols) Under Pasture in the Brazilian Cerrado." *Anais da Academia Brasileira de Ciências* 82, no. 4: 1085–1094. https://doi.org/10.1590/S0001-37652010000400026.

Webb, N. P., N. A. Marshall, L. C. Stringer, M. S. Reed, A. Chappell, and J. E. Herrick. 2017. "Land Degradation and Climate Change: Building Climate Resilience in Agriculture." *Frontiers in Ecology and the Environment* 15, no. 8: 450–459. https://doi.org/10.1002/fee.1530.

Weill, M. A. M. 1999. "Estimativa da erosão do solo e avaliação do seu impacto na microbacia do Ceveiro (Piracicaba, SP), através do Índice de Tempo de Vida." (Doctoral dissertation). University pf São Paulo.

Weng, X., B. Zhang, J. Zhu, D. Wang, and J. Qiu. 2023. "Assessing Land Use and Climate Change Impacts on Soil Erosion Caused by Water in China." *Sustainability* 15, no. 10: 7865. https://doi.org/10.3390/su15107865.

Williams, K. D., D. Copsey, E. W. Blockley, et al. 2018. "The met Office Global Coupled Model 3.0 and 3.1 (GC3.0 and GC3.1) Configurations." *Journal of Advances in Modeling Earth Systems* 10, no. 2: 357–380. https://doi.org/10.1002/2017MS001115.

Winkler, K., R. Fuchs, M. Rounsevell, and M. Herold. 2021. "Global Land Use Changes Are Four Times Greater Than Previously Estimated." *Nature Communications* 12, no. 1: 2501. https://doi.org/10.1038/s41467-021-22702-2.

Wischmeier, W. H., and D. D. Smith. 1978. *Predicting Rainfall Erosion Losses. A Guide to Conservation Planning*. Maryland: USDA Agricultural Handbook No. 537.

Wongchuig, S., J. Carlo Espinoza, T. Condom, et al. 2023. "Changes in the Surface and Atmospheric Water Budget due to Projected Amazon Deforestation: Lessons From a Fully Coupled Model Simulation." *Journal of Hydrology* 625: 130082. https://doi.org/10.1016/j.jhydrol.2023.130082.

Youlton, C., A. P. Bragion, and E. Wendland. 2016. "Eperimental Evaluation of Sediment Yield in the First Year of After Replacement of Pasture by Sugarcane." *Ciencia e investigación agraria* 43, no. 3: 374–383. https://doi.org/10.4067/S0718-16202016000300004.

Youlton, C., E. Wendland, J. Anache, C. Poblete-Echeverr'ıa, and S. Dabney. 2016. "Changes in Erosion and Runoff due to Replacement of Pasture Land With Sugarcane Crops." *Sustainability* 8, no. 7: 685. https://doi.org/10.3390/su8070685.

Yukimoto, S., H. Kawai, T. Koshiro, et al. 2019. "The Meteorological Research Institute Earth System Model Version 2.0, MRI-ESM2.0: Description and Basic Evaluation of the Physical Component." *Journal of the Meteorological Society of Japan* 97, no. 5: 931–965. https://doi.org/10.2151/jmsj.2019-051.

Zhang, J., H. Chen, Z. Fu, and K. Wang. 2021. "Effects of Vegetation Restoration on Soil Properties Along an Elevation Gradient in the Karst Region of Southwest China." *Agriculture, Ecosystems & Environment* 320: 107572. https://doi.org/10.1016/j.agee.2021.107572.

Zhu, M., W. He, Q. Zhang, Y. Xiong, S. Tan, and H. He. 2019. "Spatial and Temporal Characteristics of Soil Conservation Service in the Area of the Upper and Middle of the Yellow River, China." *Heliyon* 5, no. 12: e02985. https://doi.org/10.1016/j.heliyon.2019.e02985.

Ziehn, T., M. A. Chamberlain, R. M. Law, et al. 2020. "The Australian Earth System Model: ACCESS-ESM1.5." *Journal of Southern Hemisphere Earth Systems Science* 70, no. 1: 193–214. https://doi.org/10.1071/ES19035.

Supporting Information

Additional supporting information can be found online in the Supporting Information section.